Automatic Extraction of Retinal Disease Area for Optical Coherence Tomography Image

Mohd Fadzil Bin Abdul Kadir

System Engineering
Graduate School of Engineering
Mie University

A thesis submitted for the degree of

Doctor of Philosophy

September 2012

DECLARATION

I hereby declare that the work in this thesis is my own except for quotations and summaries which have been duly acknowledge.

10 September 2012

MOHD FADZIL BIN ABDUL KADIR
MIE UNIVERSITY, JAPAN

DEDICATION

I would like to dedicate this thesis to my mother and father, who have always loves me continuously. I am grateful to my wife, Nurshahida Binti Sallehuddin, whose patient love enabled me to complete this thesis. And not forgetting to my dearest three kids, Muhammad Nuruddin, Amatullah Maryam and Amatullah Fatimah for always be my entertainers through the hard and difficult time. I always love the three of you.

ACKNOWLEDGEMENT

Bismillahirrahmaanirrahiim

Alhamdulillah, all praises to ALLAH for the strengths and His blessing in completing this thesis.

Special appreciation goes to my supervisor, Prof. Dr. Hideo Kobayashi and Prof. Dr. Shinji Tsuruoka for their supervision and constant supports. They have devoted their valuable time and consideration to give me the needed encouragement, inspiration, guidance, suggestions and monitoring throughout the experimental and thesis works for the completion of this research.

I would like to express my appreciation to Assoc. Prof. Dr. Haruhiko Takase and Assistant Prof. Dr. Hiroharu Kawanaka for encouraging me during this study. Sincere thanks to all other colleagues and group members in the information processing laboratory of Mie University.

I would like to extend thanks to all my friends in Japan. They helped me getting through student life here.

Finally, I would like to express my appreciation to Malaysian Ministry of Higher Education, University Sultan Zainal Abidin (UniSZA), Faculty Informatics UniSZA and all people in Malaysia who give me a chance to further my studies until PhD degree.

CONTENTS

LIST OF ILLUSTRATIONS

LIST OF TABLES

ABSTRACT

Optical Coherence Tomography (OCT) is an emerging technology that can provide high-resolution cross-sectional images of the retina for identifying, and quantitatively assessing of the retinal disease. On OCT images, retinal disease area appears in two conditions, either white or black color. Quantitative information of retina is needed to evaluate the degree of disease and the effectiveness of the treatment. In the previous researches, we already proposed some automatic measurement methods of the thickness between Inner Limiting Membrane (ILM) and Retinal Pigment Epithelium (RPE) from OCT images. One of the methods used was the combination of bottom-up image processing technique and a proposed contour active net model (One Directional Active Net (ODAN)), but resulted in similar problems namely inability to extract abnormal area in some cases and inability to extract the abnormal area in white condition.

The main objective of this research is to develop a new generation computer aided diagnosis support system for OCT. The experimental materials used in this research, consists of two sets of 128 pieces of two-dimensional images of a retina. One set was obtained from a drusen patient and another set from a diabetic macular ederma (DME) patient. All of these images were digitalized to a pixel size of 6μm × 6μm, 16-bit gray scale with resolution 512 × 480 pixels. Out of 128 pieces of OCT images from each set, only 36 pieces of images which contained abnormal area were used as the final experimental materials. In this research, we used two conventional methods and proposed three new methods. At the end of the experiment, a comparison was made

between different methods of extracting the abnormal area from selected images. The results showed that a new proposed method which is border tracking procedure using regional statistics method provides the best extraction rate compared to others.

We hope that this procedure may be added in the commercial OCT unit to evaluate the degree of retinal disease suffered and enable appropriate response for treatment.

CHAPTER 1

INTRODUCTION

1.1 INTRODUCTION

The World Health Organization (WHO) reported in year 2010 that globally, the number of people from various group of ages, suffering from visual impairment is estimated to be 285 millions, of whom 30 millions are blind and 246 millions have low vision around the global. Ninety percent from the given statistics live in developing countries (Pascolini & Mariotti 2011). However, compared to the condition in last 20 years, the number of visual impairment has greatly decreased. This decline is principally the result of a reduction in visual impairment from infectious disease through concerted public health actions. Statistics data showed that there has been significant progress in preventing and curing visual impairment. Approximately 80% of all visual impairment can be prevented or cured. Progress has been made towards prevention and treatment of visual impairment through the following efforts; (WHO, 2012)

a. Governments establishing national programs to prevent and control visual impairment.

b. Eye care services increasingly integrated into primary and secondary health care systems, with a focus on the provision of services that are available, affordable and high quality.

c. Campaigns to raise awareness, including school based education.

d. Stronger international partnerships, with engagement of the private sector and civil society.

Currently, clinical doctors emphasize more development of techniques to diagnose disease at its early stages, to ensure a more effective treatment which helps in delaying and preventing irreversible damage to a patient. In ophthalmology, the precise visualization of pathology is especially critical for the diagnosis and staging of macular disease. Therefore, new imaging techniques have been developed to augment a conventional fundoscopy which examines the human retina visually. However, the conventional fundoscopy only can examines the surface of the retina. To inspect cross-sectional of retina, ultrasonic wave is used. Ultrasonography is always used in ophthalmology, but requires physical contact with the eye and has axial resolutions of approximately 200μm (Bamber and Tristam 1988). High frequency ultrasound enables approximately 20μm axial resolution, but due to limited penetration it only allows anterior eye structures can be imaged (Pavlin et al. 1992). Confocal microscopy has been used to images the cornea with sub micrometer transverse resolution (Master & Thaer 1994). Scanning laser ophthalmoscopy enables en face fundus imaging with micron scale transverse with approximately 300μm axial resolution (Webb et al. 1980; Bille et al. 1980). However, none of these techniques support high resolution, cross sectional imaging or retinal in vivo.

Recently, optical coherence tomography (OCT) has emerged as a new technique that provided high resolution and cross sectional imaging (Huang et al. 1991; Puliafito et al. 1995). OCT is attractive for ophthalmic imaging for several reasons. Among the advantages cited are, the image resolutions produced are one to two orders of magnitude higher than conventional ultrasound. Imaging can be performed non invasively and in real time, and quantitative morphometric information which can be obtained (Huang et al. 1991). OCT is similar to ultrasound, but it is uses light instead of sound. However, the most important clinical applications of OCT have been retinal imaging in ophthalmic diagnosis (Puliafito et al. 1995; Bowd et al. 2000). Details on the OCT theory are explained in Chapter 2.

1.2 PROBLEM STATEMENT

The eye is the organ of sight, a nearly spherical hollow globe filled with fluids. The retina is the light sensitive layer of tissue at the back of the inner eye. It acts like the film in a camera, and images come through the eye`s lens and are focused on the retina. The retina then converts these images into electric signals and transmitted them via the optic nerve to the brain. The color of a healthy retina is normally red due to its rich blood supply. An ophthalmoscope allows a health care provider to see through the pupil and lens to the retina. If a provider sees any changes in the color or appearance of the retina, it may indicate a disease affecting it. Retinal diseases vary widely. Some diseases are common and easily remedied, while other diseases are rare, more difficult to diagnose and require more complex treatment.

Currently, OCT is known as a noncontact high resolution technique for

obtaining cross sectional images of transparent and translucent structures. The main application field of OCT is imaging of the human retina where a lot of researches shown the diagnosis achievements of this technology (Lattanzio et al. 2001; Drexler et al. 1998).

Despite the success of OCT in retinal diagnosis applications, the technology still has, in its present state, a major shortcoming in the number of developing the useful analysis software. Diagnosis support systems or software are very important in assisting a medical doctor to evaluate and decide on a suitable process of the treatments or medications. The ability to detect the abnormal area in the OCT retinal images has potential advantages to improve methods of treatments. In order to evaluate the effectiveness of any treatment for the disease in a more precise manner, some medical doctors requires extra functions that can extract and measure the abnormal area in the OCT retinal images.

1.3 RESEARCH OBJECTIVE

The main goal of this research is to develop a new generation computer aided diagnosis support system for OCT. This particular system will extract automatically the abnormal area in the OCT retinal image that selected by the medical doctor. The research involved experimentation on OCT retinal images from human eyes using conventional and newly proposed methods. This research uses data collection and analysis from both techniques followed by the comparisons of the method used. The specific objectives of the research are as follows:

i. To identify the abnormal area by medical doctor themselves

ii. To extract the abnormal area from the OCT human retinal images.

iii. To measure the abnormal area

iv. To develop computer aided diagnosis support system for OCT images.

1.4 THESIS ORGANIZATION

This thesis consists of fives chapters in order to describe the fundamental of the works and involved activities carried out. Thesis organization follows closely to the research activities and structures. Chapter I briefly discusses the research background, the problem statements, and research objectives. The Chapter also describes organization of the thesis. Chapter II explains the background of the OCT and discusses on the human eye structures. In this chapter also, literature reviews on OCT technology and application, and related researches are presented here. Chapter III discusses the traditional methods and newly proposed methods. Data collection and data organization are highlighted in this chapter. Chapter IV presents the results of the experiments and discussions on the research findings. Lastly, Chapter V contains the summary of the research, includes the limitation of the research. Any recommendations and suggestions for the future enhancements and improvements of the newly proposed methods, also part of this chapter.

CHAPTER II

LITERATURE REVIEW

2.1 EYE STRUCTURE

Retinal locates at the back part of the eye that contains the cells that respond to light. It acts like the film in camera; images come through the eye's lens and are focused on the retina. The retina then converts these images to electric signals and sends them via the optic nerve to the brain where the electric signals are converted into images. The densely packed photoreceptor (light sensitive) cells in the macula control all the eye's central vision and are responsible for the distinguish details. The retina is usually divided into the distinct layers (Figure 2.1) including four layers of cell layers and two layers of neuronal interconnections contained ten layers (Gass 1997; Krebs & Krebs 1991). The layer of the retina starting from its inner, are as follows; (1) internal limmitin membrane, (2) nerve fiber layer, (3) ganglion cell layer, (4) inner plexiform layer, (5) inner nuclear layer, (6) outer plexiform layer, (7) outer nuclear layer, (8) external limiting membrane, (9) photoreceptor layer, and (10) retinal pigment epithelium. The

most common of functional blindness or ocular disease is breakdown of the macula. Damage to the macula results in the lost, either partial or complete, of ability to see objects clearly in the center of vision. Although not totally blind, the person has difficulty performing tasks and continue pursue some normal daily activities without assistance.

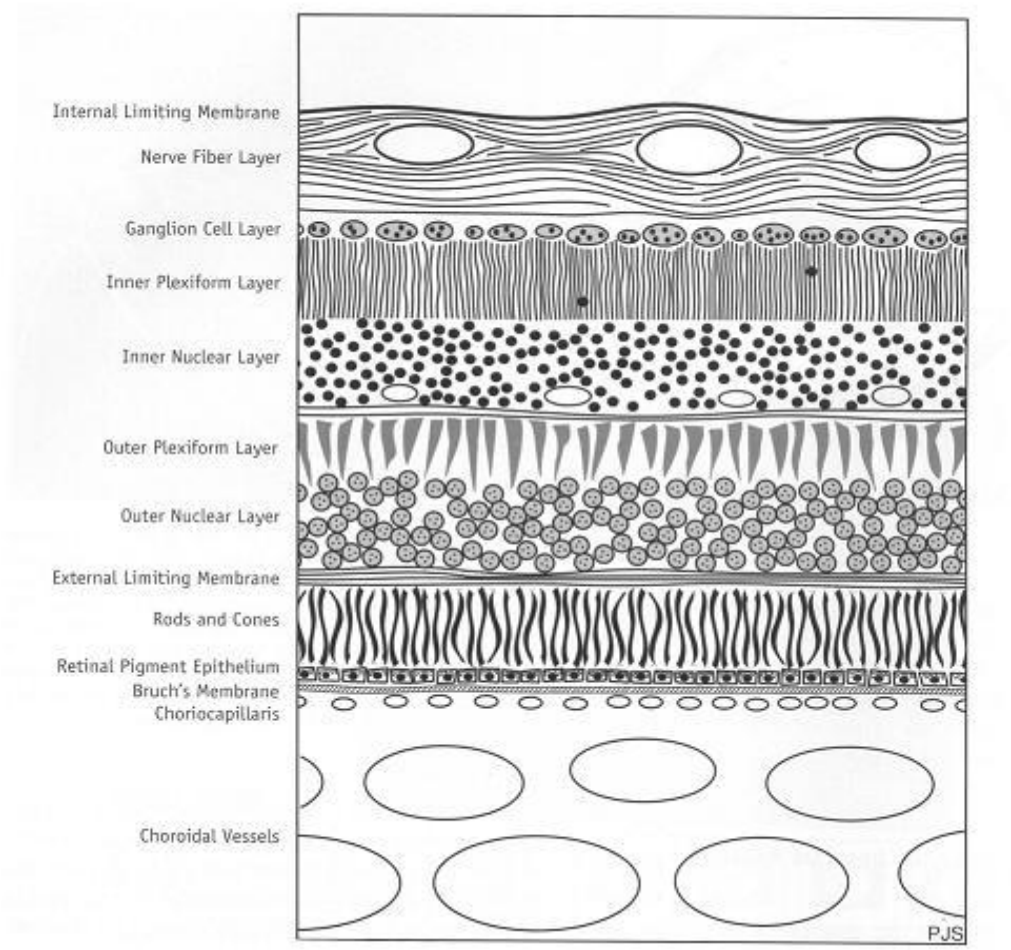

Figure 2.1: Retinal layer (taken from www. http://telemedicine.orbis.org)

2.2 OPTICAL COHERENCE TOMOGRAPHY (OCT)

Optical coherence tomography (OCT) is a new technique of optical imaging

technology. In ophthalmology, OCT can perform high resolution, cross sectional imaging of retinal morphology. The quantitative morphometric information of retina can be obtained in order to assessing the retinal diseases. Imaging can be performed in real situation and real time with one to two orders of magnitudes finer than conventional ultrasound. OCT imaging is similar to conventional ultrasound imaging except it uses light instead of sound. The unique features of OCT make it become a powerful technology, which promises to enable many fundamental research and clinical applications.

Recently, optical coherence tomography (OCT) has emerged as a promising new technique for high-resolution, cross-sectional imaging. OCT is attractive for ophthalmic imaging because image resolutions are 1-2 orders of magnitude higher than conventional ultrasound. Imaging can be performed non-invasively, in real time. There are several different methods for performing OCT, but essentially imaging is performed by measuring the magnitude and echo time delay of back-reflected or back-scattered light from internal microstructures in materials or tissues. OCT images are two dimensional data sets, which represent optical back-reflection or back-scattering in a cross sectional plane.

As mentioned above, interference lies at the core of the OCT imaging method. One of the two signals is the interfere signal in internal as the reference beam, and the other one, is the reflected signal reflected by the target, as the object beam. Different interferometer configuration also can be used in OCT.

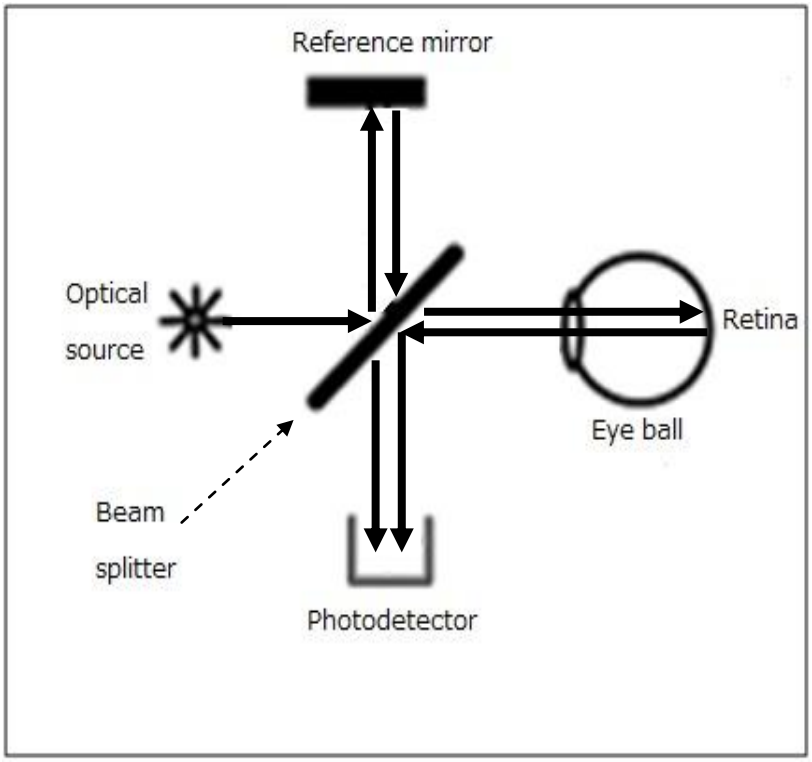

Figure 2.2: Principle of OCT

Figure 2.2 illustrates the principle of OCT. The light from swept source is divided into two beams by using a plate beam-splitter. Light exiting the reference fiber is incident upon a reference delay and redirected back into the same fiber. Light exiting the sample fiber in incident upon a scanning mechanism designed to focus the beam on the sample and to scan the focused spot. The light back-scattered or back-reflected from the sample is directed back through the sample optical scanning system into the sample arm fiber, where it is mixed with the returning reference arm light in the fiber coupler, and the combined light is made to interfere on the surface of a photo detector or receiver. The interfered amplitude is arrayed as two dimensional data, and cross-sectional grayscale image is generated (Figure 2.3).

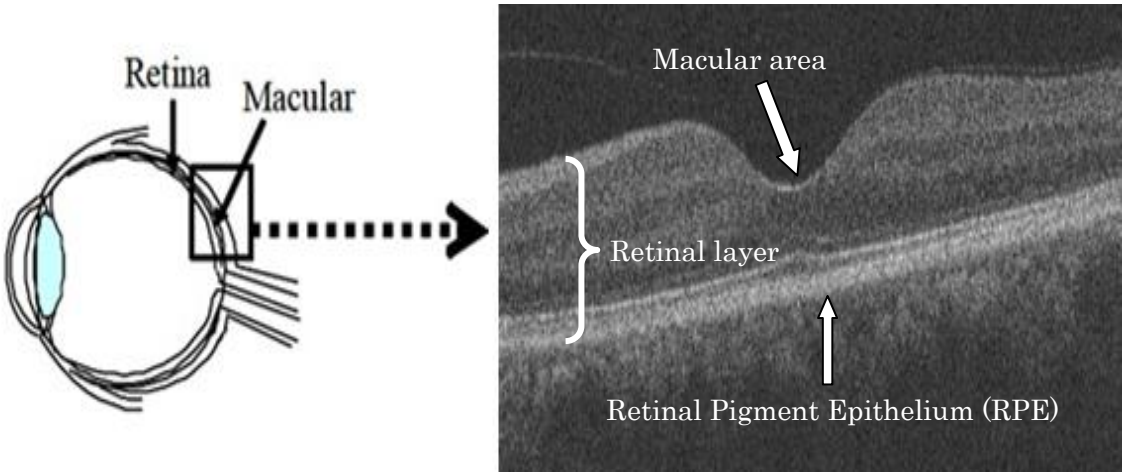

Figure 2.3 Structure of eye and OCT image

2.3 OCT IN OPHTHALMOLOGY

OCT is a powerful technology in ophthalmology because it can identify early stage of the retinal disease before physical symptoms and irreversible vision loss occurs. Furthermore, the quantitative information by repeated imaging can be performed to track disease progression or monitor the effectiveness of treatments. The technology was introduced commercially for ophthalmic diagnostics to the market in 1996 by Carl Zeiss Meditec (Swanson 2009). Current ophthalmic OCT system is now accepted as a standard of care in ophthalmology and is consider essential for the diagnosis and monitoring of many retinal disease as well as glaucoma (Fercher 1996; Schuman et al. 2004). However, the most important clinical applications of OCT have been retinal imaging in ophthalmic diagnosis (Bowd et al. 2000).

The development of OCT in ophthalmology proceeded rapidly. In ophthalmic imaging, the high detection sensitivity of OCT enables imaging structures such as retina.

Hence, high depth resolution is an important feature for any imaging technique used to diagnose retinal pathology. The first in vivo retinal images were obtained in 1993 (Fercher et al. 1993). The potential of OCT in diagnostic imaging of retinal disease was proven in 1995 (Puliafito et al. 1995) and in the same year, the application of OCT to high resolution imaging of the normal human retina was demonstrated (Hee et al. 1995). At present, OCT provides axial resolution of 2–3μm represents a significant advance in performance over the 10–15μm resolution currently available in ophthalmic OCT systems. This resolution is the highest resolution for in vivo ophthalmologic imaging achieved to date (Draxler et al. 2001). Many retinal diseases are accompanied by changes in retinal thickness. The thickening of the retinal nerve fiber layer may be an important indicator for early glaucomatous changes (Zeimer et al. 1998). By using image processing techniques and OCT images, retinal thickening caused by retinal diseases such as macular edema or glaucoma (Schuman et al. 1995; Zaimer et al. 1998) and its layers could be estimated quantitatively. Quantitatively measurements of the retinal thickness and its layers are of particular importance in the assessment of retinal diseases.

In a retinal diagnosis using OCT, light beam from optical source is directed onto the retina to be imaged. The back reflected light produced by the accident with the retinal layer contained interference beam. The retinal OCT images generated by scanning the reflected beam, producing two-dimensional data set displayed as a gray scale image (Fujimoto et al. 2000; Huang et al. 1991). The generated images (Figure 2.3) show the structure of retinal morphology at an intra-retinal level. The precise visualization of retinal structure morphology is the most critical in diagnosis ocular disease. Therefore the needs of retinal imaging using OCT devices have been growing

(Drexler et al. 2001).

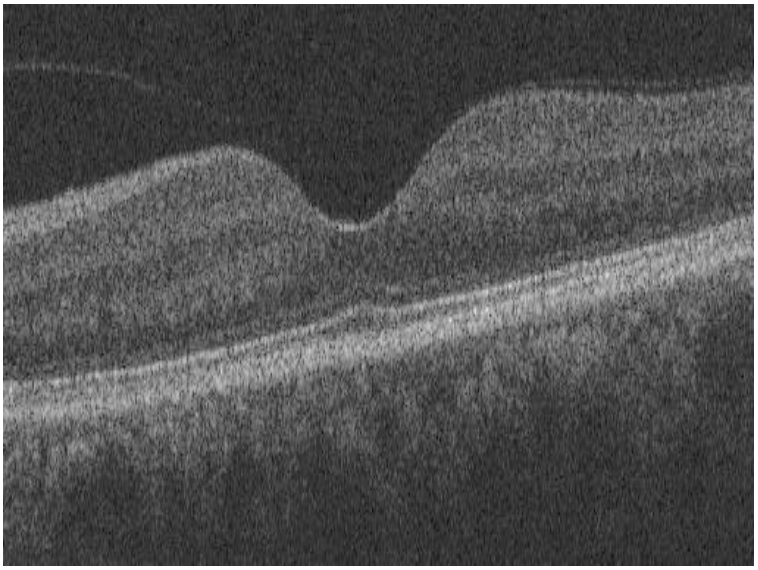

Figure 2.4 OCT image for normal retina

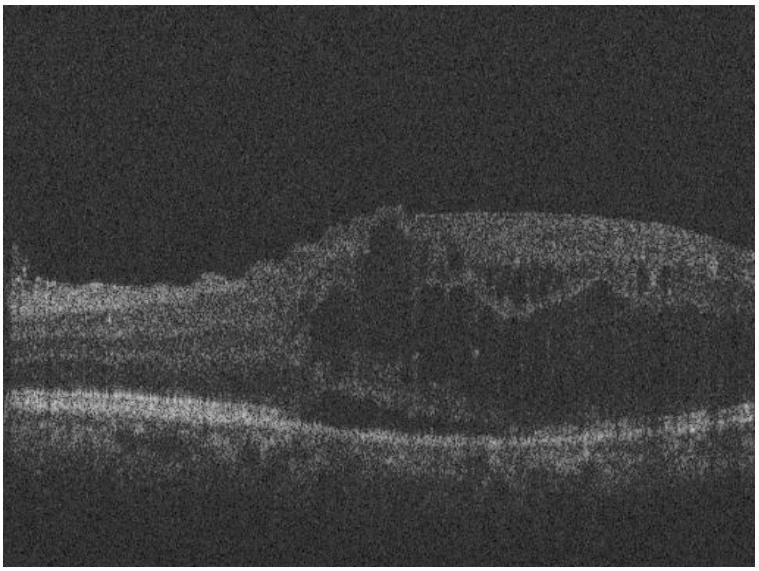

Figure 2.5 OCT image for abnormal retina

Abnormal area in the retinal can exist in two conditions, either black or white color when scanned using OCT machine. Figure 2.6 shows the abnormal area in black

condition and Figure 2.7 shows the abnormal area in white condition.

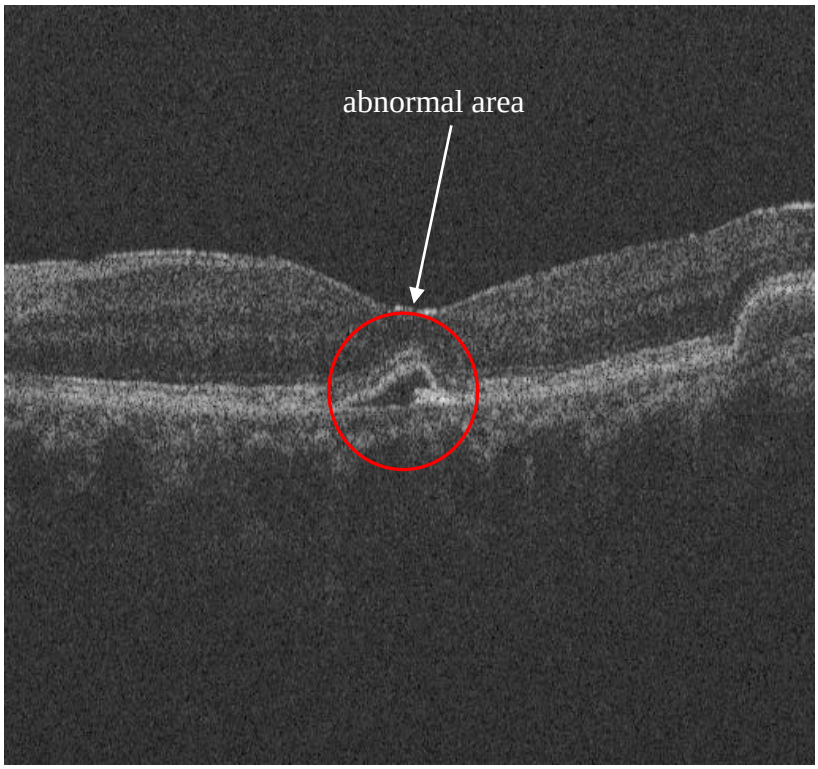

Figure 2.6 Abnormal area existed in black condition

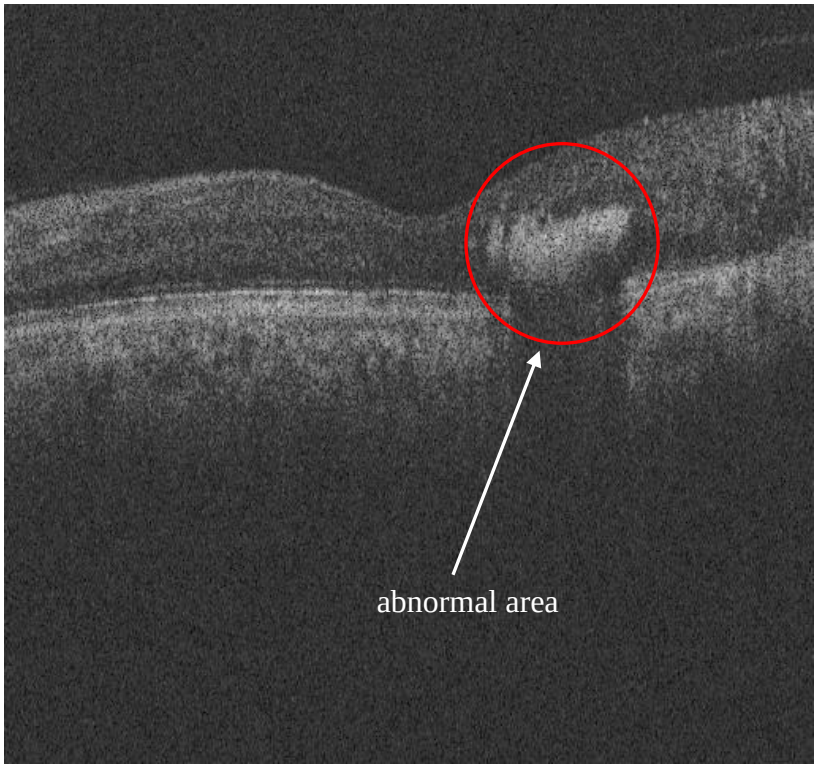

Figure 2.7 Abnormal area existed in white condition

Quantitative information on retinal thickness between inner limiting membrane layer (ILM) and retinal pigment epithelium (RPG) (Tony et al. 2005) and abnormal area in the retinal can be used to assess the retinal disease and also the process of treatment. The extraction method of the thickness between inner limiting membrane and retinal pigment epithelium using morphological technique has been done in 2008 (Yagi et al. 2008). This method used bottom up approach to detect the layers of inner limiting membrane and retinal pigment epithelium. Even though this method can extract both layers for normal retinal OCT image, it has a problem in detecting the both layers in abnormal retinal OCT image. This method also cannot extract very well to some OCT images contained large noises. To improve Yagi`s method, one directional active net (ODAN), which is one of the dynamic contour model employs a new energy function to

extract automatically the inner limiting membrane layer and retinal pigment epithelium layer (Yamakawa et al. 2010). Active net (Sakaue & Yamamoto 1991) is based on the energy minimization theory and all nodes of ODAN move to vertical direction. The results showed that the ODAN can improves Yagi`s method. Figure 2.8(a) and Figure 2.8(b) show the result that the ODAN method can extract the layers in both normal and abnormal OCT images.

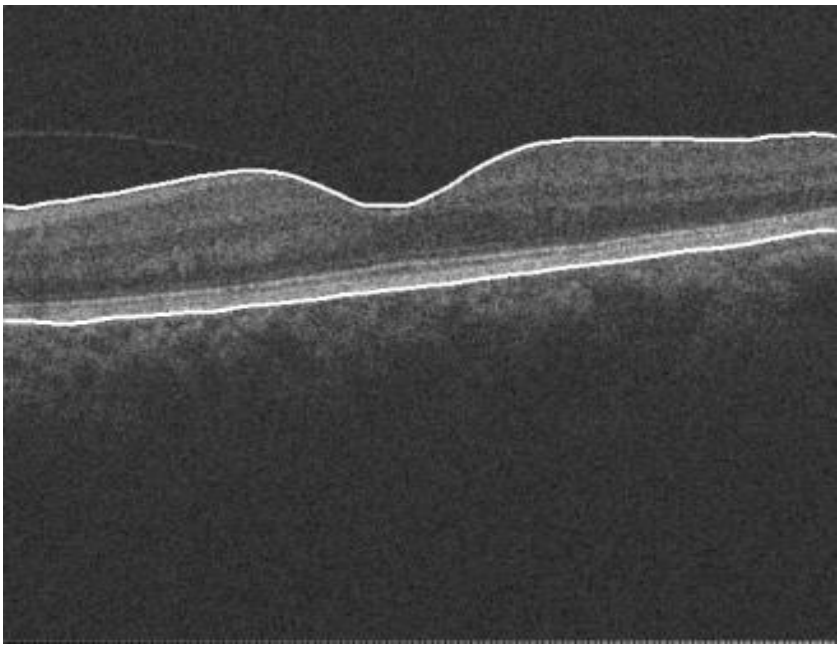

(a) Normal retina

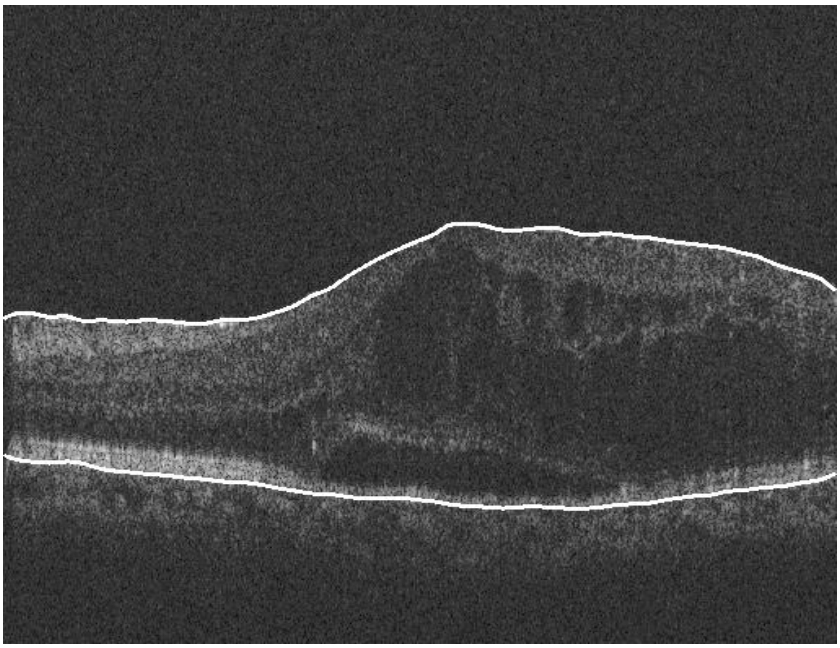

(b) Abnormal retina

Figure 2.8 Extracted border using ODAN

As explained before, human`s retina contains ten layers. The structure images of the retinal layers were shrunken or broken by the existed disease. The number of layer boundaries will decrease at the abnormal area. The analysis to evaluate the size of retinal disease by calculating the number of retinal layers (Kodama et al. 2010) takes too much time around 5.33sec per OCT image. However Kodama`s method only can detect the abnormal area in white color condition and cannot extract the actual size of retinal disease but only the disease size in horizontal direction. All of these three methods also have the same problems which are:

i. They cannot extract the abnormal area itself, which mean can extract only the retinal thickness.

ii. They cannot extract the layer`s border if the retinal border in damage condition.

iii. They cannot extract the abnormal area in white condition.

Conventional extraction methods evaluate the retinal disease and treatment effectiveness by measure the thickness of retinal layer. In this research, I used two conventional methods and proposed three newly extraction methods that only extract the abnormal area in the retinal images. These methods will give more precise results and can reduce the processing time.

CHAPTER III

RESEARCH METHODS

3.1 METHODOLOGY

This chapter describes the experimental methods applied to extract the abnormal area from OCT retinal images. Five different methods were used including two conventional methods to extract the abnormal area and record the processed images. The images were analyzed and processed using Microsoft Visual C#.NET on Windows and embedded into graphical user interface (GUI). Figure 3.1 shows the GUI of the system. Upon completion of all experiments, the percentages of extraction from the different methods were compared to ascertain the most appropriate method which can provide the best result. The experimental materials used in this research, consists of two sets of 128 pieces of two-dimensional images of one retina. One set was obtained from a drusen patient and another set from a diabetic macular ederma (DME) patient. All of these images were digitalized to a pixel size of 6μm × 6μm, 16-bit gray scale with resolution 512 × 480 pixels. Out of 128 pieces of OCT images from each set, only 36

pieces of images which contained abnormal area were used as the final experimental materials. The experiment focused only on the abnormal area at macula part because this is the important part in the human retina controlled all the eye`s central vision (Visionrx 2005). In the proposed system, the abnormal area in the image was identified by a medical doctor selects an abnormal area by pointing at the interested area (abnormal area) using a computer mouse. The selected pixel is known as an initial pixel.

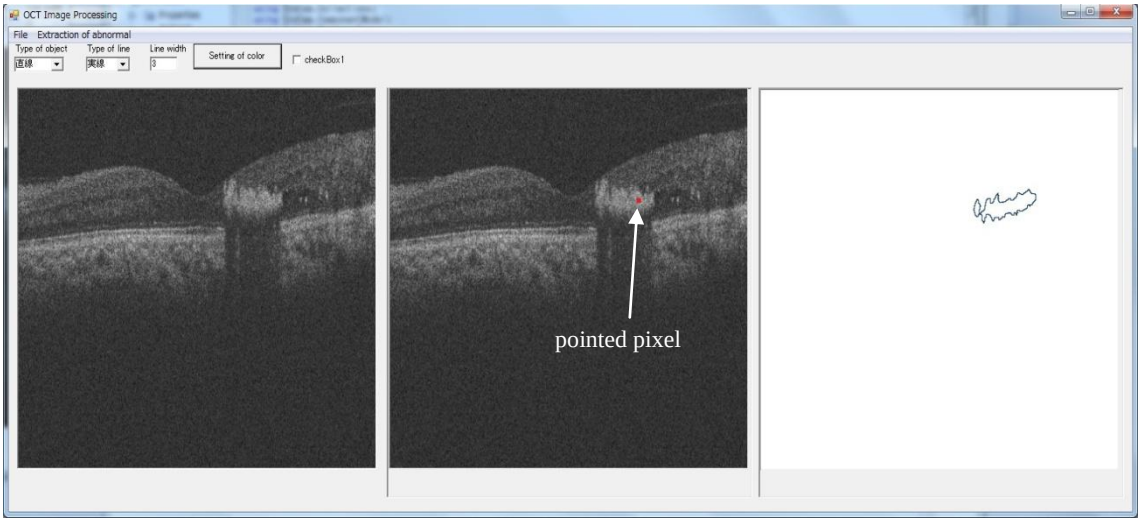

(a) OCT image (b) Pointing a pixel in abnormal area by computer mouse (c) Extracted border of the abnormal area

Figure 3.1 GUI of proposed system

3.2 IMAGE SCANNING METHOD

This method is one of the conventional methods that was used in the experiment. The original OCT image of retina (Figure 3.2) was inserted into input side. Generally, the raw OCT images contain speckle and spike noise due to multipath reflection and interference in the retinal layer. A smoothing process was applied to OCT image as a preprocessing. The smoothing process employed the median filter of 3 × 3

pixels (Figure 3.3). Figure 3.4 shows the example of smoothed image using 3 × 3 median filter. For certain types of random noises, median filters provide excellent noise reduction capabilities, with considerably less blurring than linear smoothing filters of similar size (Gonzalez & Woods 2002). As its name implies, replace the value of a pixel by the median of the gray levels in the neighborhood of that pixel:

$$\hat{f}(x, y) = \text{median}_{(s,t)\in S_{xy}}\{g(s,t)\} \qquad (3.1)$$

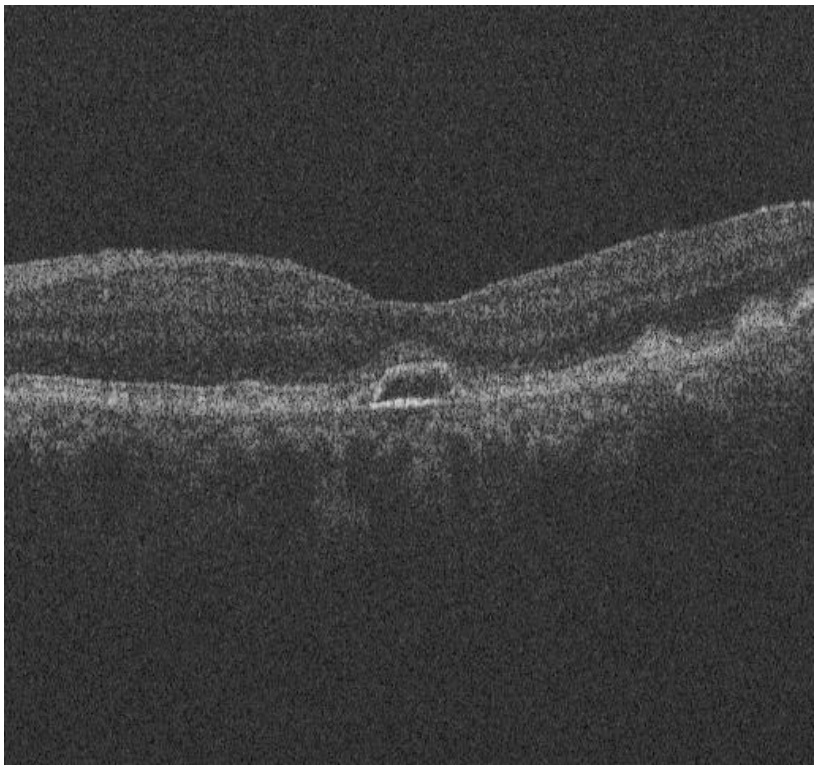

Figure 3.2 Original OCT image of human retina

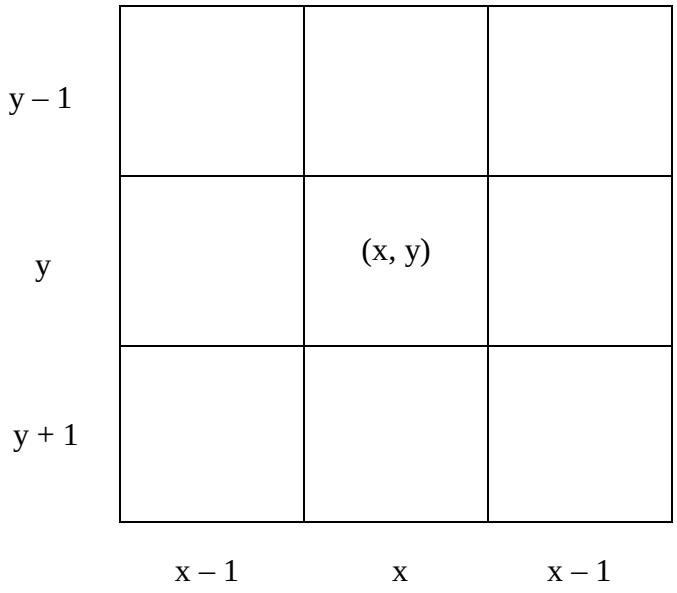

Figure 3.3 Neighbors of a pixel (x, y)

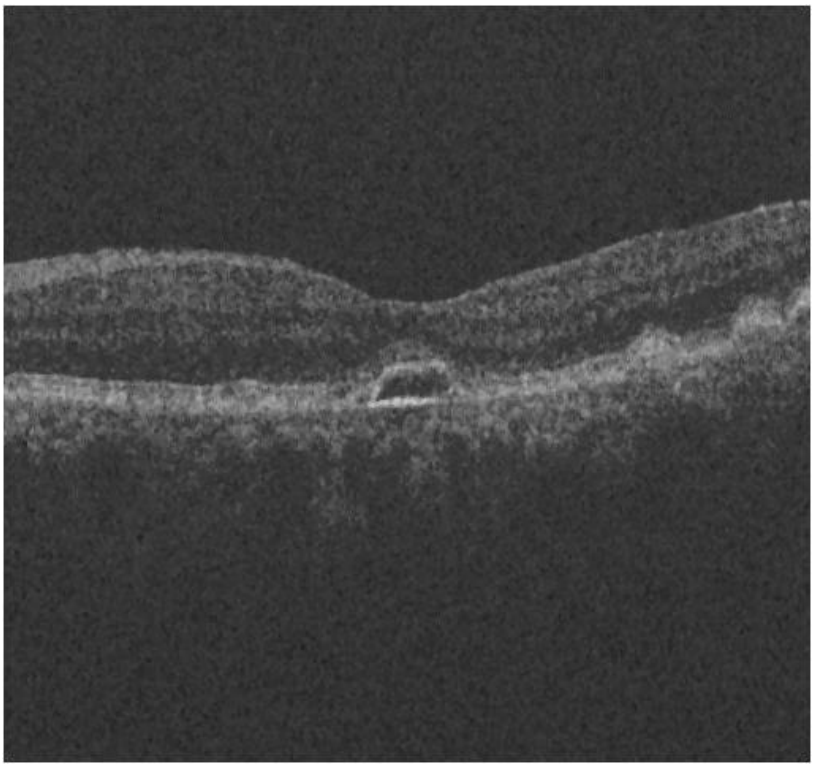

Figure 3.4 Result of OCT smoothing image using median filter

A binarization process then was applied to the smoothed image. Image binarization is typically treated simply as a thresholding operation on a grayscale image. This process is known as image thresholding and the output image is known as binary image. Only two colors are used for the binary image, black and white though any two colors can be used. The formula for binarization is denoted by the expression

$$g(x, y) = B[f(x, y)] \tag{3.2}$$

$$g(x, y) = \begin{cases} 1 & \text{if } f(x, y) \geq B \\ 0 & \text{Otherwise} \end{cases} \tag{3.3}$$

where f (x, y) is the input image

g (x, y) is the processed image

B is binarization threshold of f.

Figure 3.5 shows the binary image after the binarization process. The binary image shows that the intensity of the most pixels in the neighborhood or retinal image changed to white color.

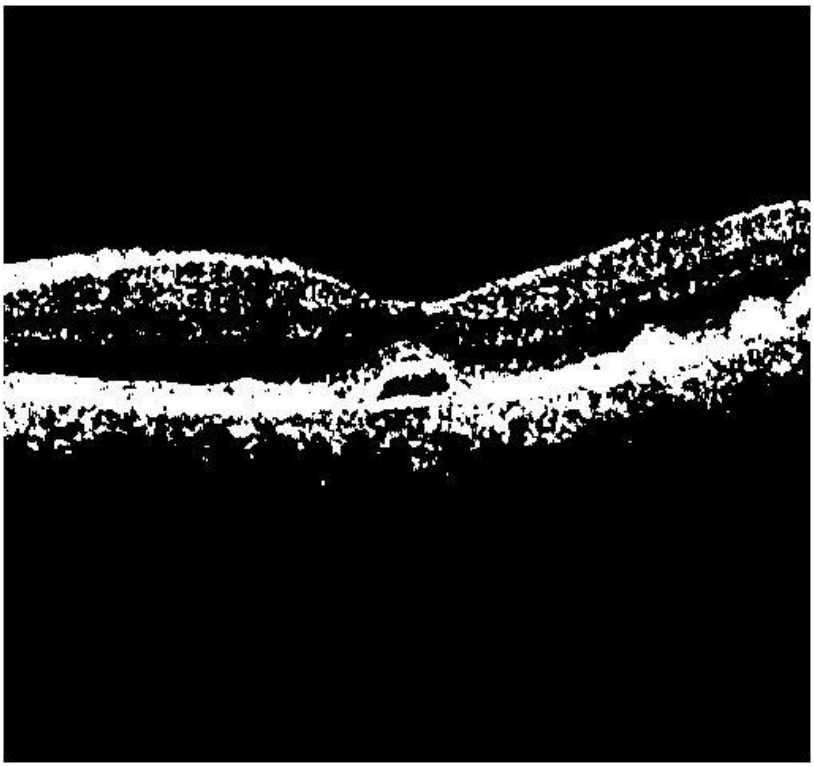

Figure 3.5 Binary image

Scanning process is employed as the next step of this method. First, the system scanned the image started from the initial pixel pointed by the medical doctor. The system scanned all the same color of the initial pixel one-by-one in four direction ways; upper-right, upper-left, down right, and down left until it traced at the different color from initial pixel (see Figure 3.6). The color in the scanned area not changed, however the image outside of the scanned area is changed to white. The final result (Figure 3.7) only shows the extracted abnormal area from OCT retinal image.

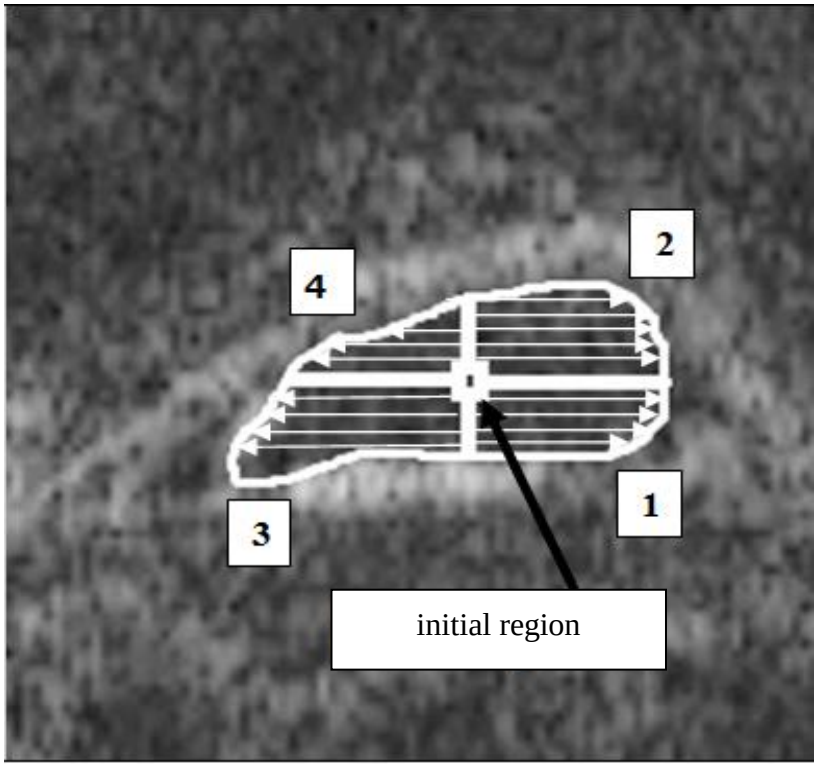

Figure 3.6 Image scanning process for each pixel in binary image

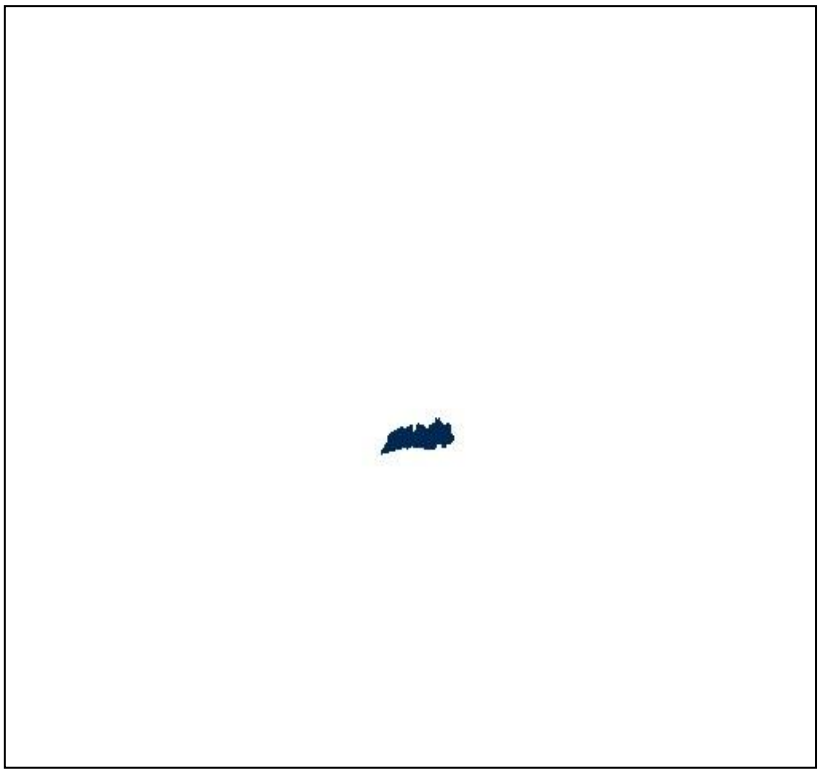

Figure 3.7 Extracted area from Image Scanning Method

3.3 BORDER TRACKING EXTRACTION METHOD

This method is another one of the conventional methods which is applied in this experiment. In this method, the boundary extraction of abnormal area in OCT retinal image were extracted pixel by pixel from the same region from a connected component. The most efficient way of coding group membership for regions in images is to code the boundary of the area or region containing the pixels (Rao et al. 2009). Note that in this research, binary 1's are shown in white and 0`s in black and the normal treatment of this method is to assume that values outside the borders of the image are 1. Eight chain-code (Figure 3.8) scheme for the border (Kouichi 2007) was used in this method for representing boundaries of image regions. In this coding scheme, the orientation of an edge is quantized along eight discrete directions.

4	3	2
5	x	1
6	7	8

Figure 3.8 Eight chain-code

There are four steps were applied to extract the abnormal area using this method (Figure 3.9). The first three steps are similar with the first method (Image Scanning Method).

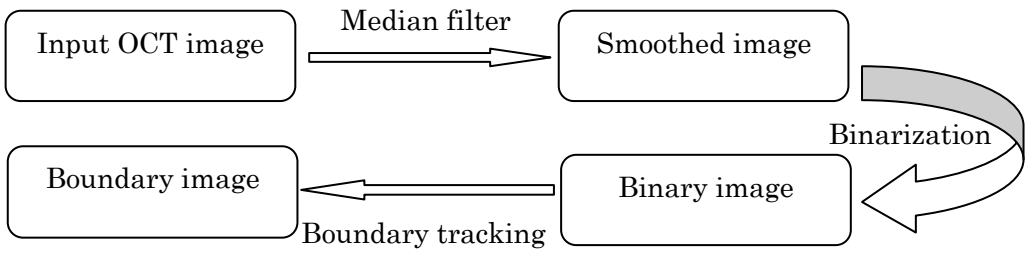

Figure 3.9 Block diagram of border tracking method

Boundary tracking was applied at the last step of the method. Figure 3.10 (enlarge at the abnormal area of Figure 3.5) shows the steps of border tracking.

Step 1: The initial pixel selected by medical doctor is moved forward to the top of the image one by one pixel. The moving pixel stopped when the system detected the different color between the moving pixel and the initial pixel.

Step 2: A starting pixel is the last moving pixel after the system traced the white pixel. The system scans the border of abnormal area from the starting pixel to the end.

Figure 3.11 shows the example of border tracking image.

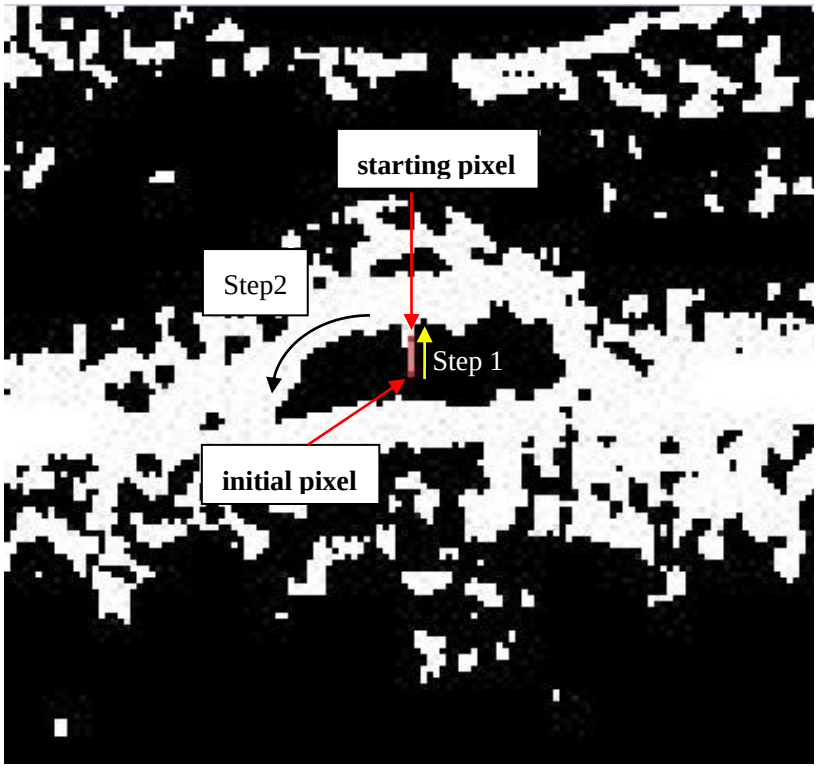

Figure 3.10 Procedure of border tracking

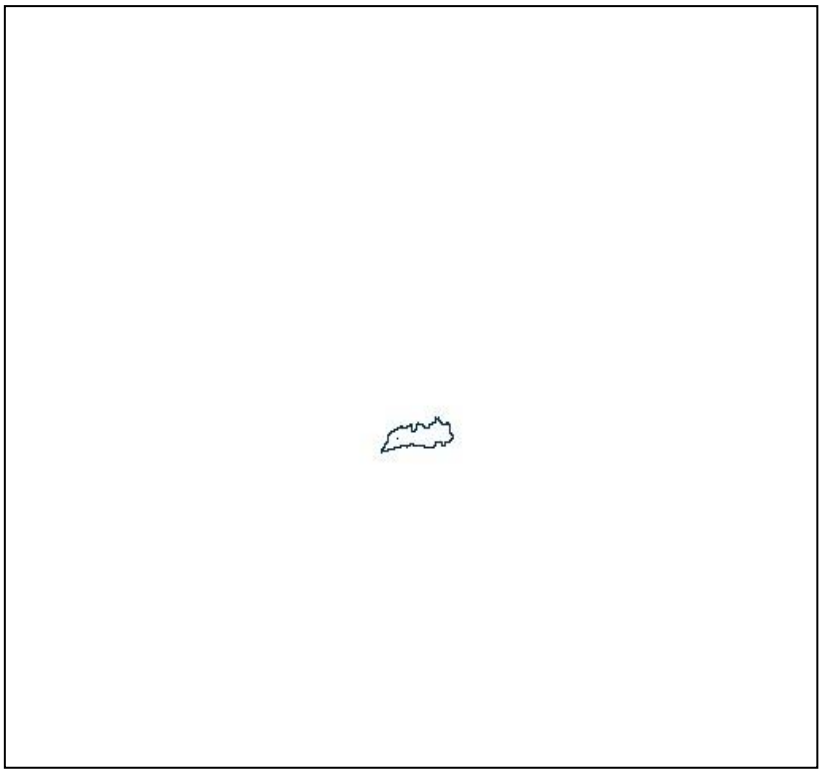

Figure 3.11 Border tracking image

3.4 STATISTICS BORDER TRACKING METHOD

Under this method, direct comparisons between the gray value of moving pixel and the mean μ ± the standard deviation σ, of gray value of the initial pixel. The mean and the standard deviation of the gray level in neighborhood 5 × 5 (Figure 3.12) of the pixels that surrounded the selected pixel (initial pixel) will be calculated to be set as a benchmark value.

$$(\mu - a\sigma) < f(i, j) < (\mu + a\sigma) \qquad (3.4)$$

where μ is the mean

σ is the standard deviation

a is the constant

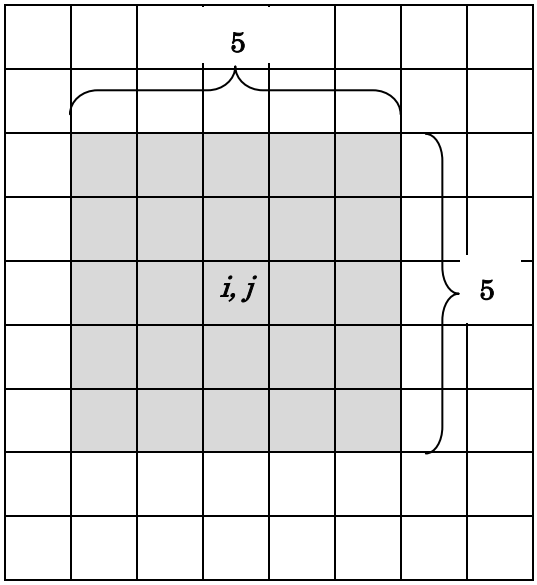

Figure 3.12 Initial pixel (*i*, *j*) and neighborhood 5 × 5

The scanning process started from the top the image. The system scans all the pixels to calculate the gray value of the pixel to compare with the equation (3.4). If the gray level value is in the range of equation (3.4), it changes to 1 or white color. Otherwise, it changes to 0 or black color. The process will scan all the pixels to the end of the image and gives the output in binary image (Figure 3.13) format.

To extract the border line of the image, the processes are similar to the Border Tracking Extraction Method. The moving pixel moves one by one from initial pixel up forward to the top of the image until the system traces the different color between the moving pixel and the initial pixel. Border tracking process is applied to the binary image to give the final result as border tracking image (Figure 3.14).

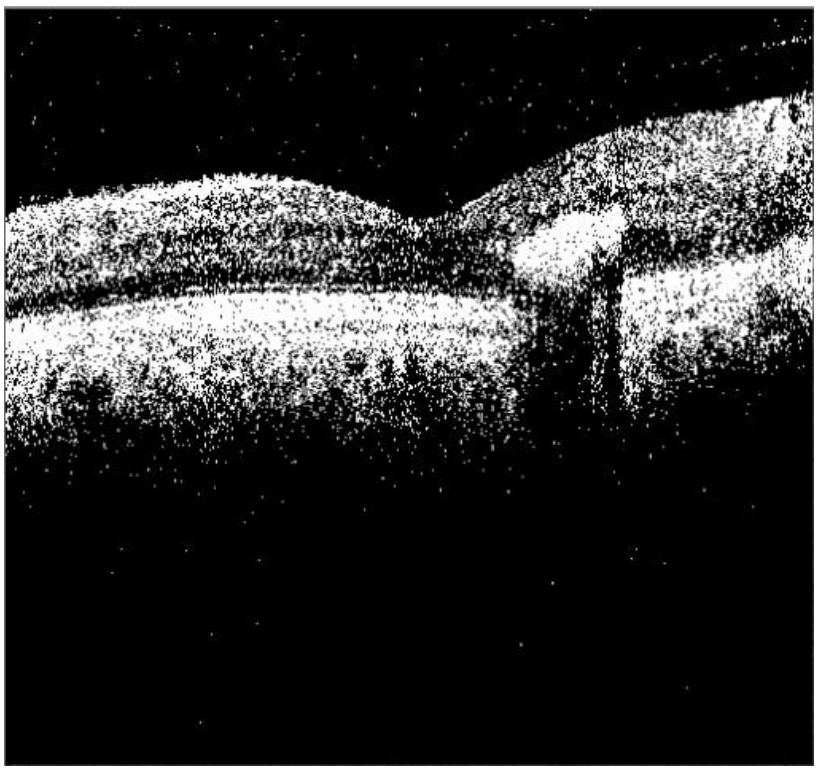

Figure 3.13 Binary image using Statistics Border Tracking Method

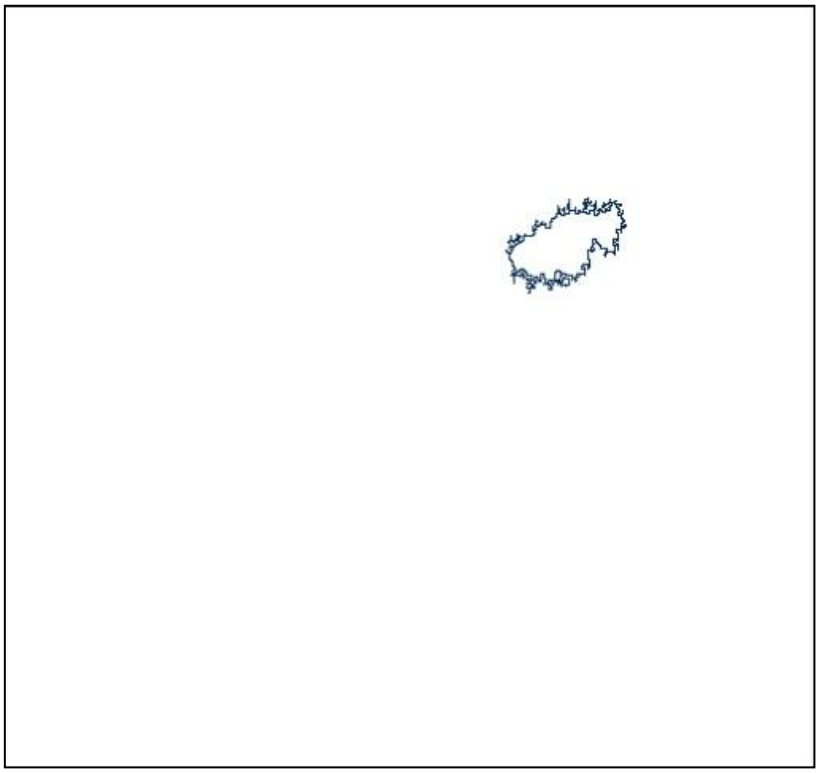

Figure 3.14 Border tracking image

3.5 REGIONAL STATISTICS AREA EXTRACTION METHOD

In this method, the system will extract the abnormal areal form retinal OCT images using regional statistics technique. Initial region defined as 25 (5 × 5) pixels that surrounding the initial pixel, *i* (Figure 3.11). The standard deviation σ of gray level of initial region is calculated

$$\text{Standard Deviation } \sigma = \sqrt{\frac{1}{25}\sum_{n=1}^{25}(\mu - x_n)^2} \qquad (3.6)$$

Where x_n is the gray level of each pixel.

μ is the mean where $\mu = \sum_{n=1}^{25}(x_n)/25$ (3.7)

The standard deviation values of the initial region used in the equation (3.8) as a benchmark.

$$(\sigma - a\sigma) < \sigma_x < (\sigma + a\sigma) \qquad (3.8)$$

Where σ_x is standard deviation of moving region

a is the variable.

The center of the 25 pixels (initial pixel *i, j*) will moves to next pixel (*i + 1, j*) on the right movement and to be a new center of the second region surrounding by new 25 pixels (Figure 3.15). A new value of standard deviation σ_x will calculate and compare with the equation (3.8). If the calculated standard deviation value meet the condition of equation (3.8), the center of moving region will moves one by one pixel until the standard deviation of the moving region not meets the condition in given equation (3.8).

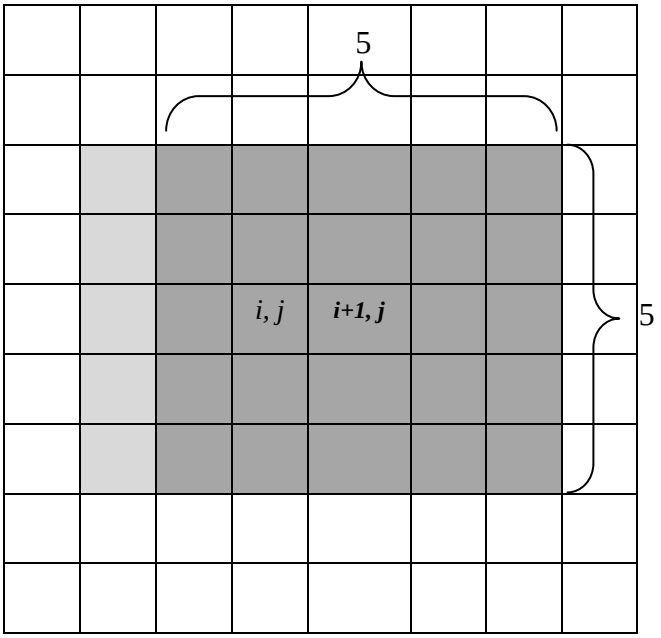

Figure 3.15 Moving region and *i + 1* as a new center of the region

These steps will repeat in four ways (see Figure 3.6) on the right-down, right-up, left-down, and left-up to extract the abnormal area in the OCT image (Figure 3.16).

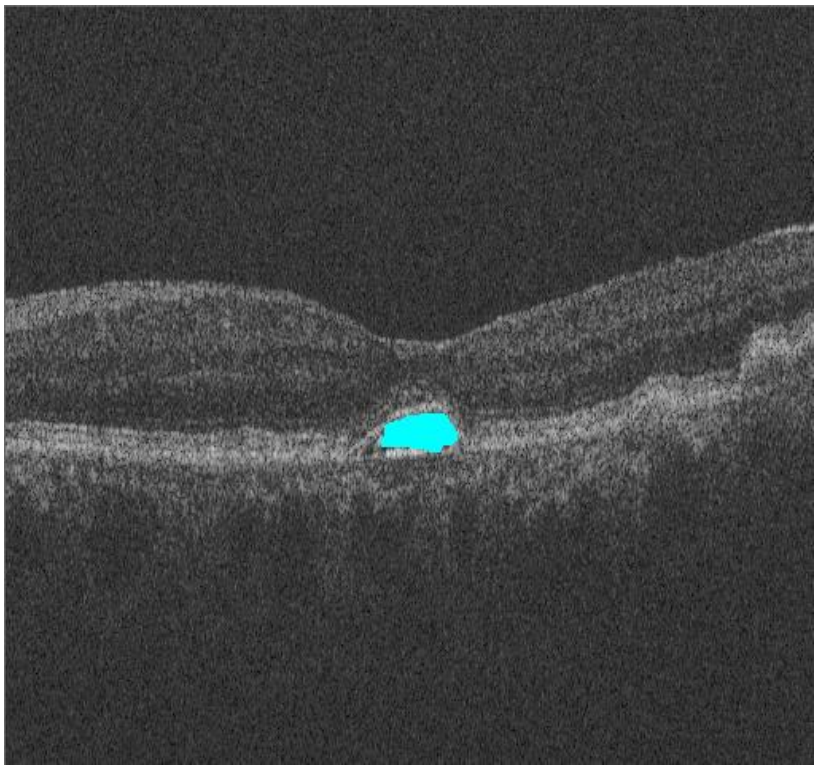

Figure 3.16 Extracted image

Figure 3.17 shows the flowchart of all the process in regional statistics area extraction method.

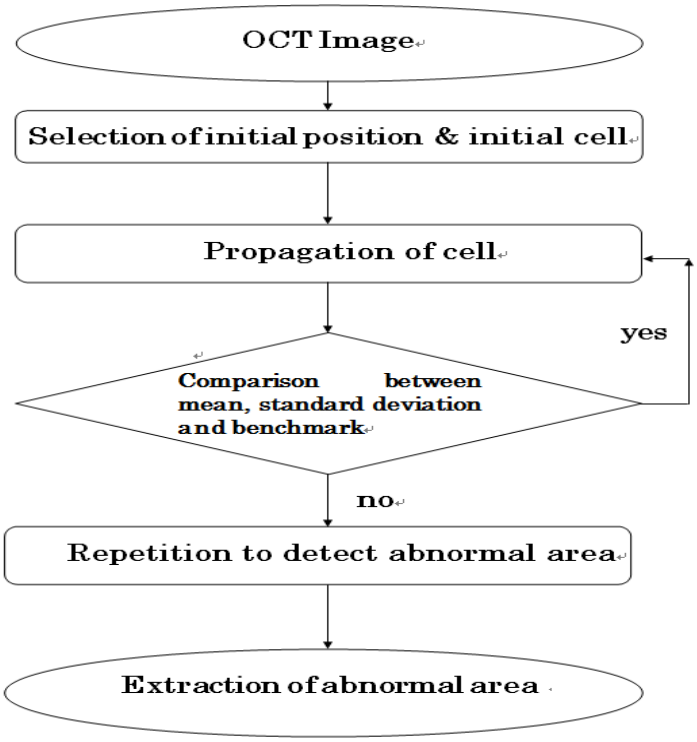

Figure 3.17
Flow chart of the regional statistics extraction method.

3.6 BORDER TRACKING PROCEDURE USING REGIONAL STATISTICS

In this method, a medical doctor needs to select the region of interest by clicking at a using computer mouse. Figure 3.18 shows the initial pixel selected by the medical doctor is marked with red square. The initial region is defined as 25 pixels (5 × 5 pixels) surrounding the initial pixel (Figure 3.12). The mean μ and standard deviation σ of gray level pixel in initial region were be calculated and stored in program memory.

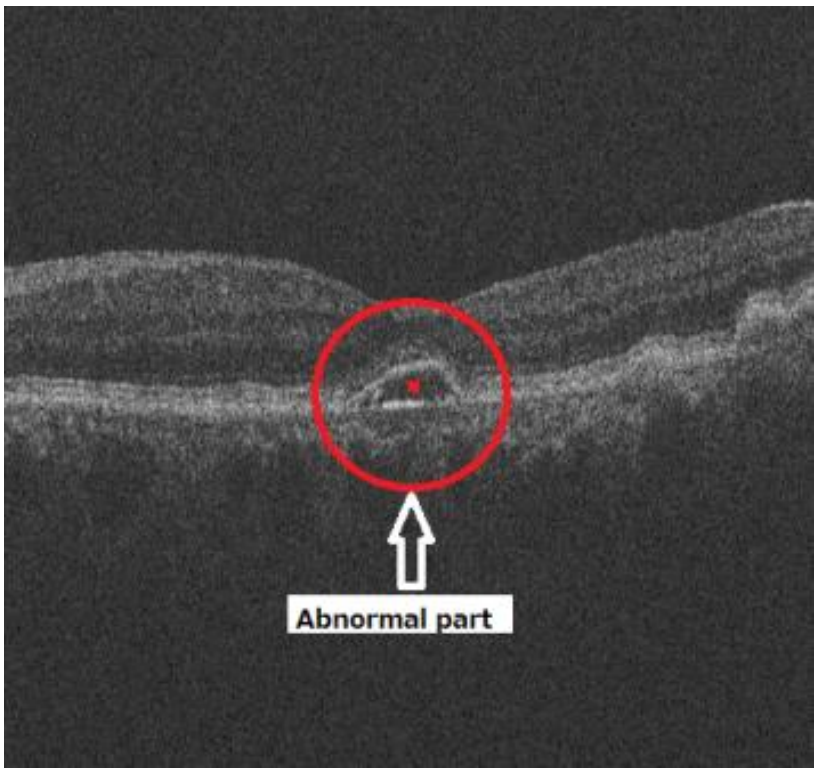

Figure 3.18 Initial pixel (red square)

The calculated values of mean and standard deviation were used to generate threshold formula. Then, the system calculates mean μ_x or all moving regions and determines that every pixel are belonging to abnormal area or not using equation (3.9).

$$(\mu - a\sigma) < \mu_x < (\mu + a\sigma) \qquad (3.9)$$

Where a is the constant.

μ_x is mean of region.

μ is mean of initial region.

σ is standard deviation of initial region.

If the calculated mean μ_x meet the condition of Equation (3.9), the system will changes the gray value of center pixel of moving region to value 255 or white, otherwise the

gray value changes to 0 or black. The system scanned all the region from top to bottom of the OCT image to change to binary image (Figure 3.19).

Figure 3.19 Binary image

From the initial pixel (*i, j*) the scanning process to detect the abnormal area border is initiated. The position of the next pixel was determined by moving the initial pixel (*i, j*) to the next pixel (*i, j-1*) toward the top of the image. The system scanned the pixel one by one until it traced the gray level value of the moving pixel as different from the gray level value of initial pixel. The border extraction process will used eight chains-code algorithm (Figure 3.8) to extract the abnormal area border. Figure 3.20 shows the extracted border tracking image.

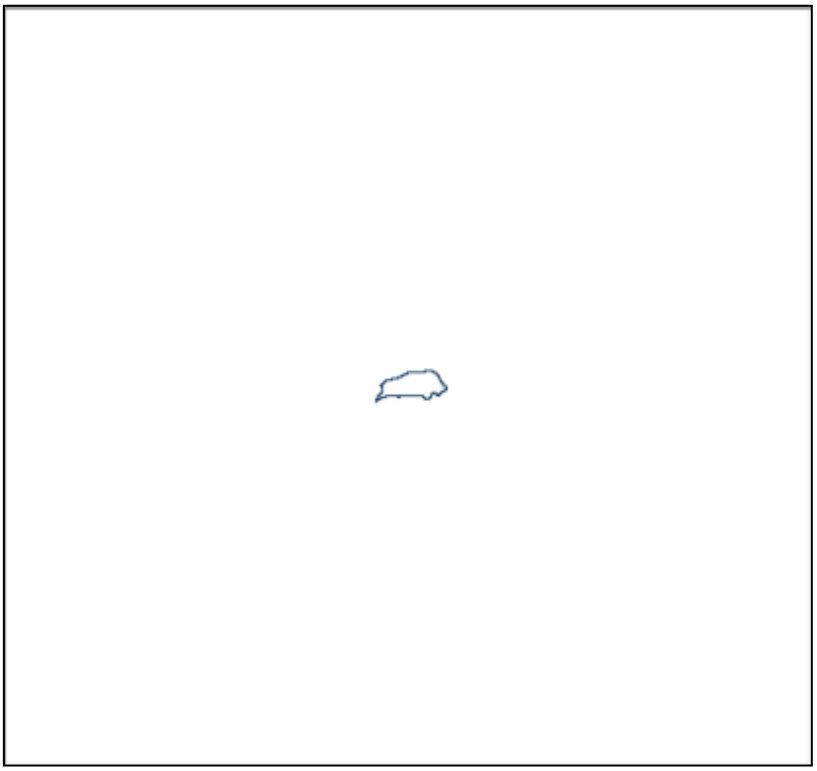

Figure 3.20 Border tracking image

CHAPTER IV

RESULT AND DISCUSSION

This research was used 36 pieces of OCT images from a single retina of a drusen patient and 35 pieces of OCT images from a single retina of a diabetic macular edema (DME) as materials of the experiment. These images were clearly showed the abnormal area at the macular part.

4.1 IMAGE SCANNING METHOD

The first step of this method was smoothing processed in digital image processing. This processed was employed the 3 × 3 medial filter. The next process is binarization hat was applied to smoothed image. Binary image that contained two colors black and white only was provided. The last step was the system extracted the abnormal area automatically that selected by the medical doctor.

From the experiment, the system was extracted only 41.7% from the provided images. This meant, only 15 pieces of OCT images were extracted their abnormal area properly. This data shows in Table 4.1.

Table 4.1 Performance of successful extracted area by image scanning method

OCT Image (pieces)	Extracted	Failed	Successful rate %
36	15	21	41.7

The following images are examples of the output results by applied this method on the OCT retinal images.

Figure 4.1 Original OCT retinal image

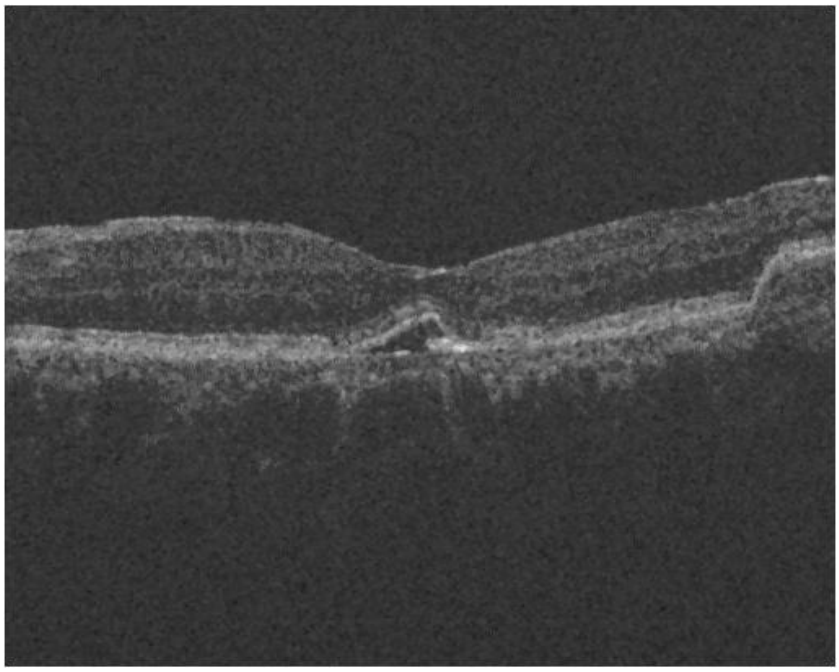

Figure 4.2 Smoothed OCT retinal image using 3 × 3 medial filter

Figure 4.3 Binary image

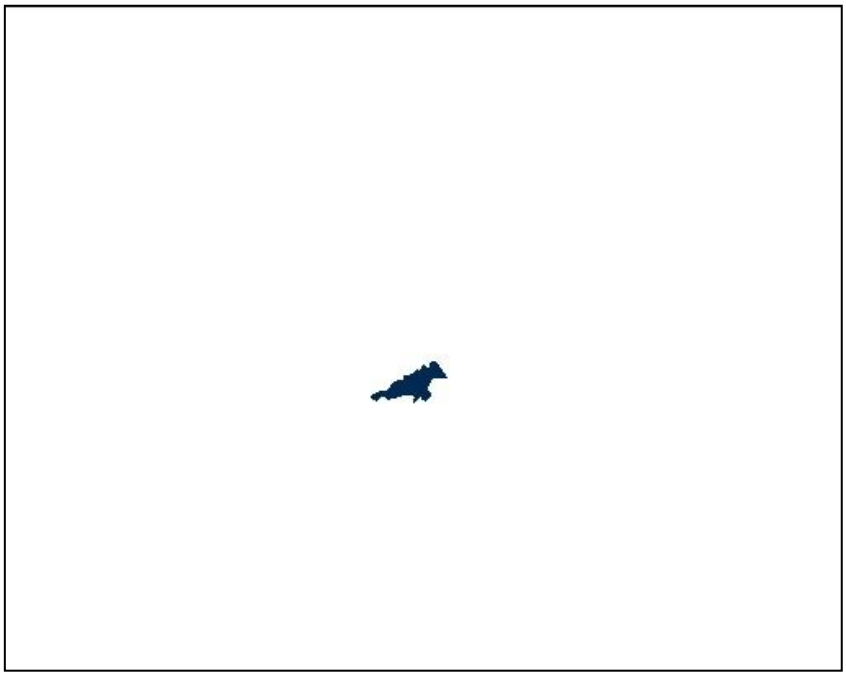

Figure 4.4 Extracted image

Figure 4.5 Original OCT retinal image

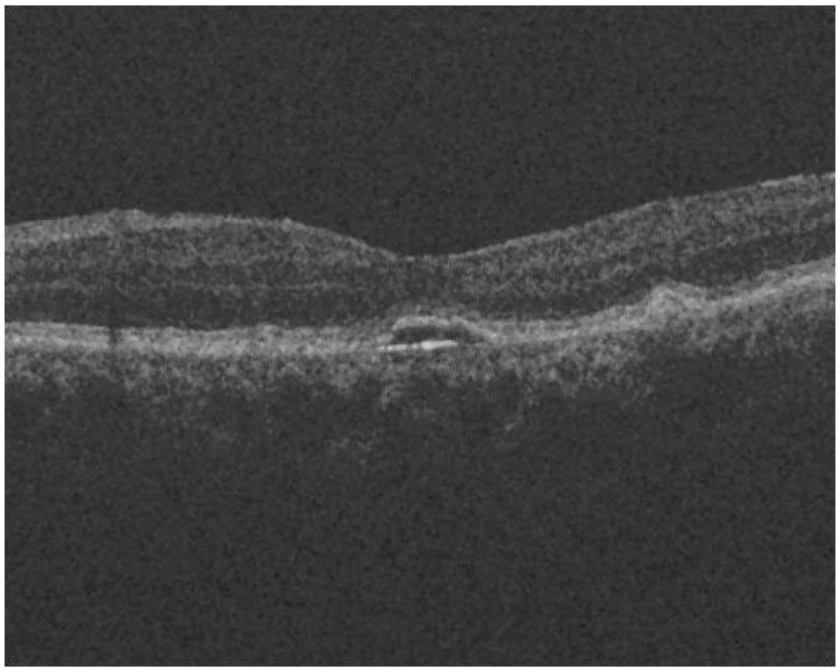

Figure 4.6 Smoothed OCT retinal image using 3 × 3 medial filter

Figure 4.7 Binary image of Figure 4.6

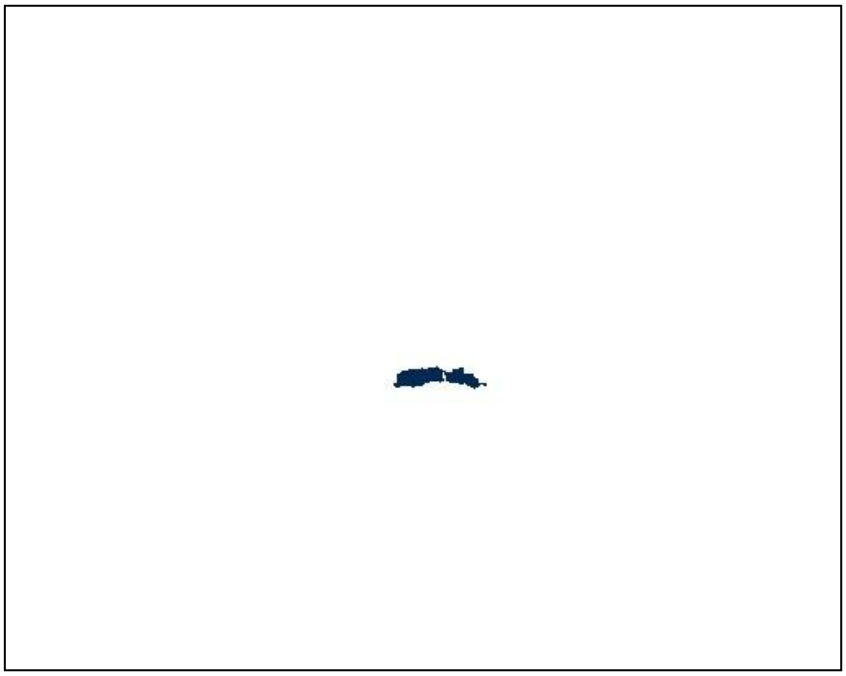

Figure 4.8 Extracted abnormal area from Figure 4.7

Figure 4.4 and 4.8 are the example of the successful extracted image.

Figure 4.1 to 4.4 show the output image of each process using this method. The original OCT retinal image was taken from material number 67 of the supplied materials. All these images show that the method can extract properly from the beginning.

The original image of Figure 4.5 to 4.8 was taken from material number 73 from supplied materials. These examples show that the method can extract the abnormal area properly from the beginning. From these examples, the method could be extracted the abnormal area if the original image in the proper and perfect condition.

As the early mention in the Chapter II, OCT retinal image can exist in two conditions. First, the abnormal area appears in black condition and the second is abnormal area appears in the white condition. Due to this method, the experiment was extracted the abnormal area in black condition only. There were also some errors or the

system cannot extract the abnormal area properly. One of the reasons was the damage of the retinal layer existed in the OCT image. Figure 4.9 to Figure 4.12 shows the example of his problem. Figure 4.9 does not show clearly the damage, however when the method changed the original image to binary image (Figure 4.11), the damage clearly appear at the retinal layer.

Figure 4.9 Original OCT image

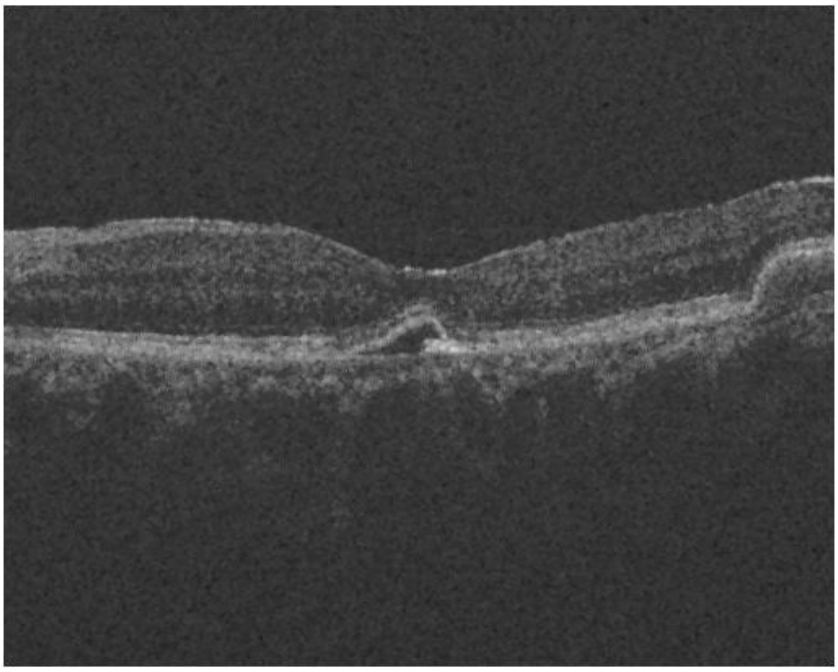

Figure 4.10 Smoothed OCT retinal image using 3 × 3 medial filter

Figure 4.11 Binary image

Figure 4.11 shows that the damage layer appeared when the image changed to binary image.

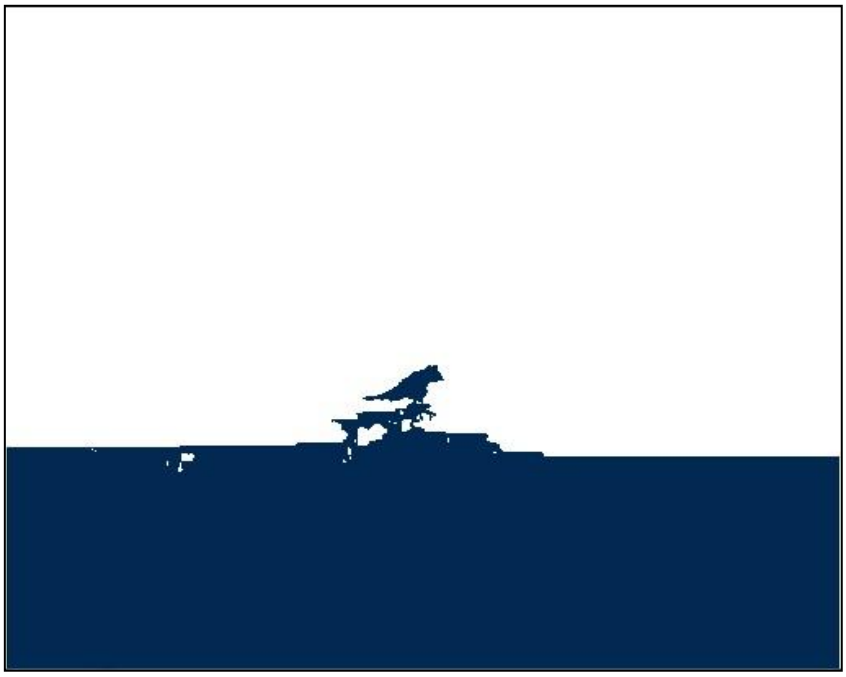

Figure 4.12 Failure example - retinal layer in damage condition

The system cannot extract abnormal area properly when the retinal layer was contained damaged in OCT image (Figure 4.12).

This method also cannot extract the abnormal area when abnormal area separated into two parts. Figure 4.13 to Figure 4.16 show about this problem.

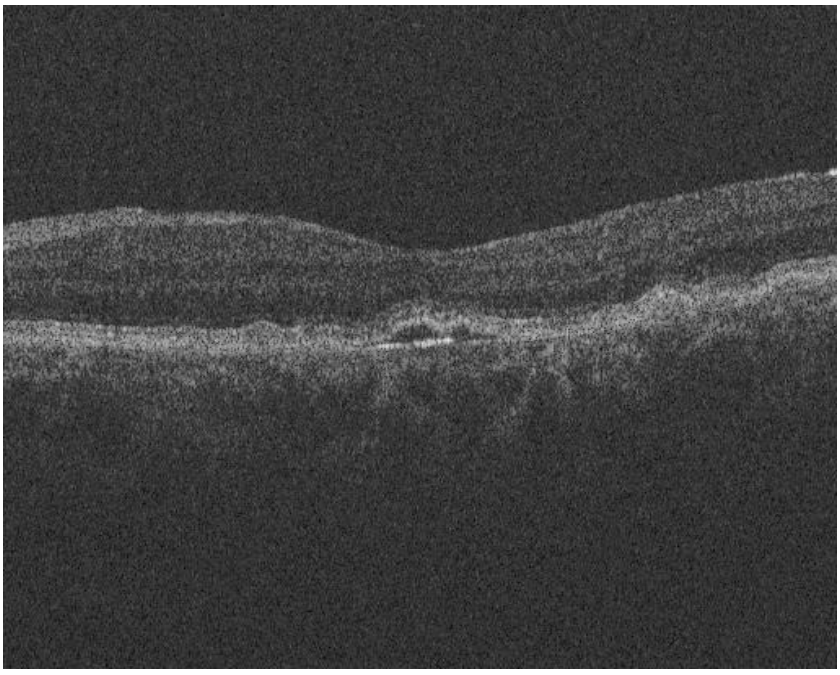

Figure 4.13 Original OCT retinal image

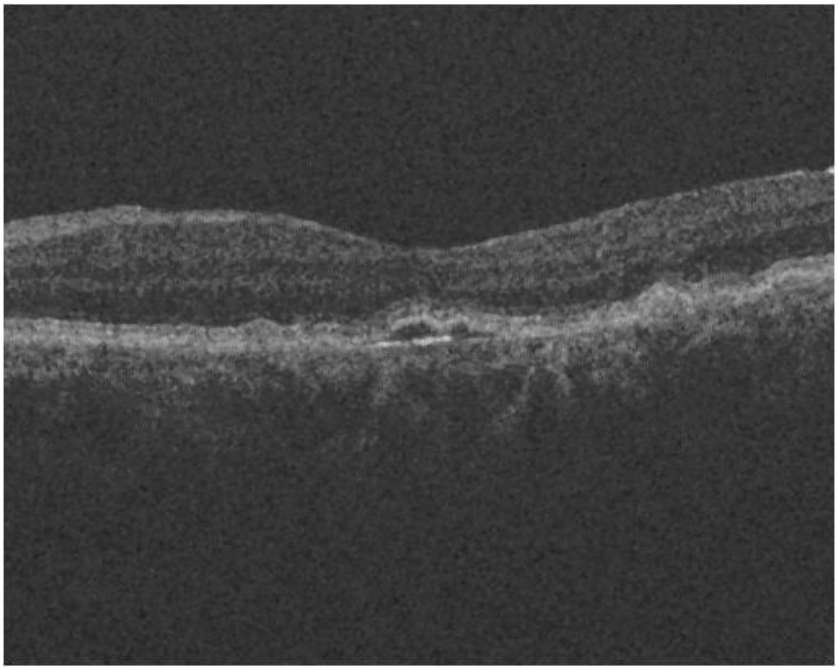

Figure 4.14 Smoothed OCT retinal image using 3 × 3 medial filter

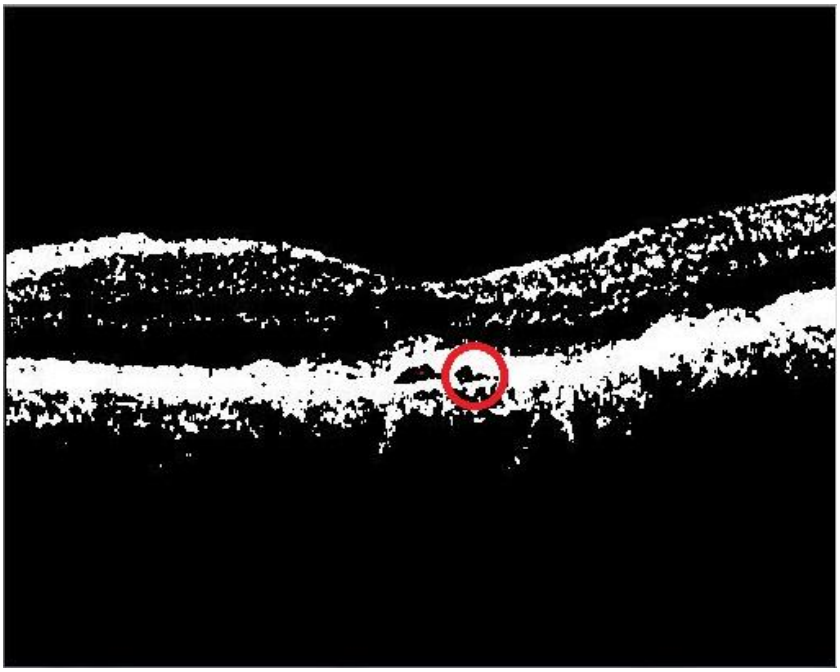

Figure 4.15 Binary image

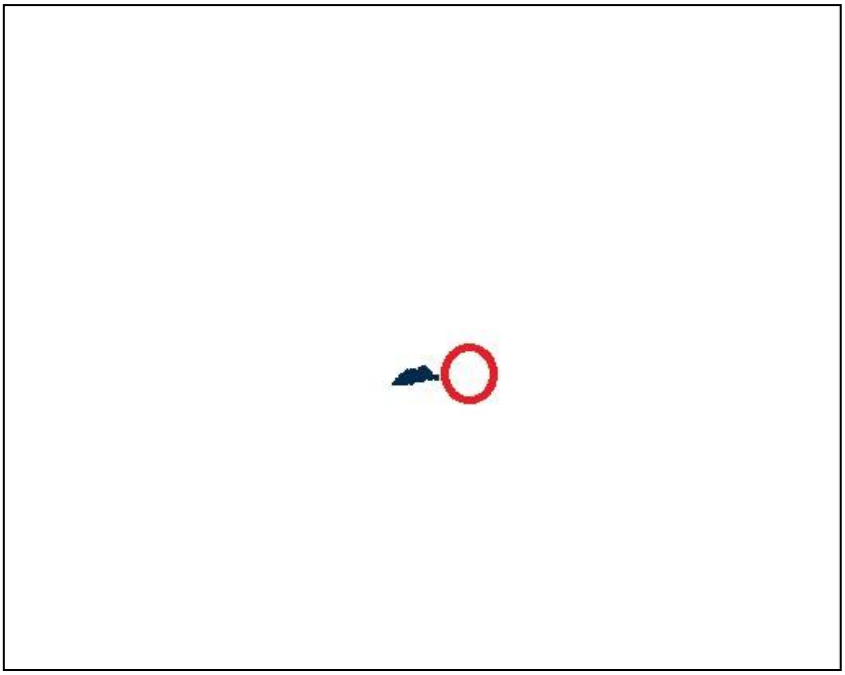

Figure 4.16 Failure example - abnormal area divided into two parts

Abnormal part in the original image divides into two parts. When the system processes

the image, this method only extracted the abnormal area that selected by medical doctor without another part of abnormal area shows in the red circle (Figure 4.16).
The experiment shows that this method cannot extract properly the image that contained damages at retinal layer.

4.2 BORDER TRACKING EXTRACTION METHOD

This method used eight chain-code. The orientation of an edge is quantized along eight discrete directions as explained in Chapter II. From the experiment, the method was extracted only 41.7% from the provided images. That is meant; only 15 pieces of OCT images was extracted their abnormal area properly. This data shows in Table 4.2.

Table 4.2 Performance of successful extracted abnormal area using border tracking method

OCT Image (pieces)	Extracted	Failed	Successful rate %
36	15	21	41.7

The percentage successful rate of border tracking method was the same with the result of image scanning method. This is because these two methods was used the same technique to change the original images to binary image. These two methods also, used the smallest element of pixel (one pixel) to extract the abnormal area or abnormal area`s border. Below are some of the output results by applied this method on the OCT retinal images.

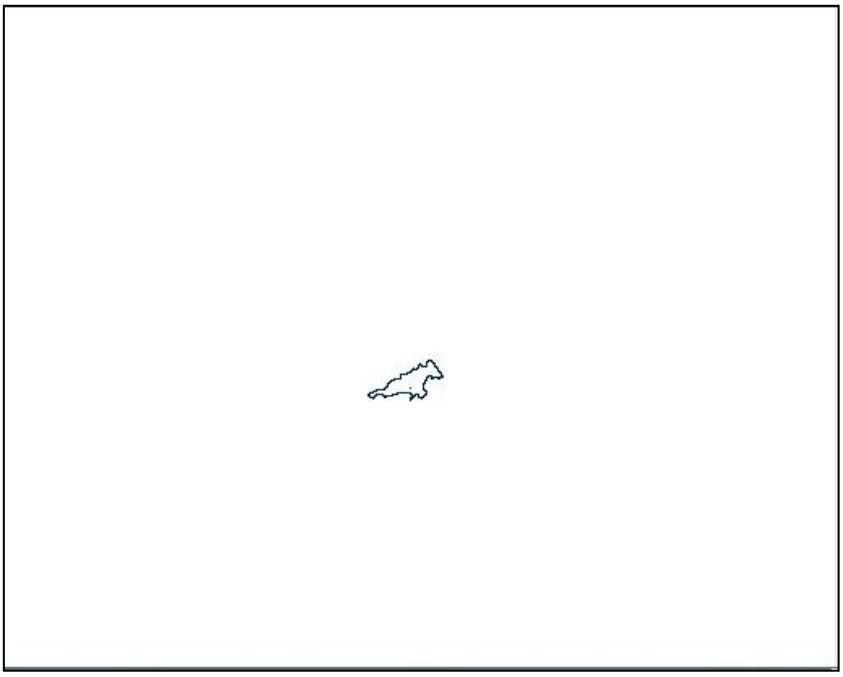

Figure 4.17 Border extracted image

Figure 4.17 shows the extraction border image that extracted from the material number 73 from the supplied images. The original image was the same image (Figure 4.1) that used in the image scanning method above. The smoothed image and binary image in this method also the same with smoothed (Figure 4.2) and binary image (Figure 4.3). The system provided better extraction result when the original OCT retinal images were in good condition.

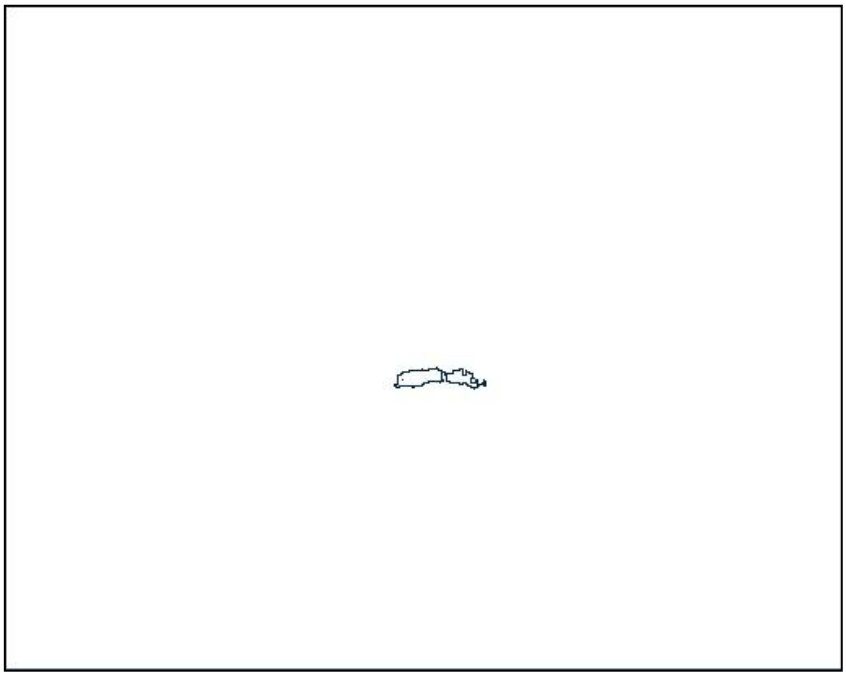

Figure 4.18 Border extracted image

Figure 4.18 shows the border extracted image by using border tracking method. This image was taken from material number 67 from the supplied experiment material. The original image was the same with image that used in the image scanning method (see Figure 4.5). The smoothed image and binary image in this method also same with smoothed (Figure 4.6) and binary image (Figure 4.7). The system provided better extraction result when the original OCT retinal images were in good condition.

Because of border tracking method used the same theory (smallest element of pixel or single pixel) in smoothing, binarization, and extracting border process with image scanning method, the problem that facing in this method also same. Border tracking method cannot extract the border of abnormal area that existed in two parts (Figure 4.19). Figure 4.20 shows that this method cannot extract properly the abnormal area on the OCT images that contained damages at the retinal layer.

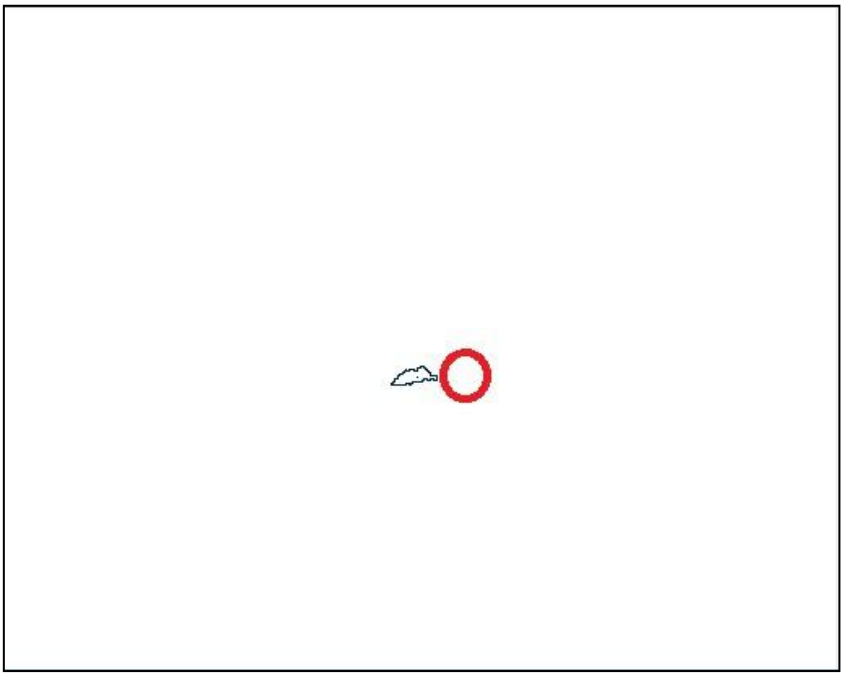

Figure 4.19 Failure example – abnormal area divided into two parts

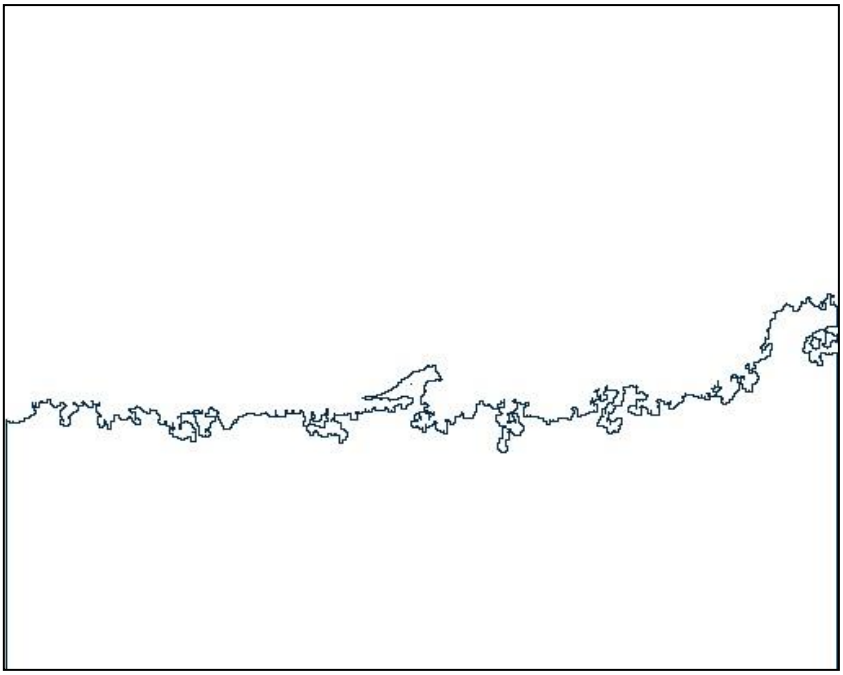

Figure 4.20 Failure example – retinal layer in damage condition

4.3 STATISTICS BORDER TRACKING METHOD

In this conventional method, binary images were extracted directly from original OCT image without change to smoothed image. This method was proposed to counterpart the original OCT retinal image that the abnormal area existed in white condition problem. From the experiment, the method was extracted only 57.1% from the provided images. That is meant; only 20 pieces of OCT images was extracted their abnormal area properly. These data show in Table 4.3.

Table 4.3 Performance of successful extracted abnormal area using statistics border tracking method

OCT Image (pieces)	Extracted	Failed	Successful rate %
35	20	15	57.1

Statistics border tracking method can extract the abnormal area in white condition in the OCT retinal images. Figure 4.21 shows the example of original OCT retinal image that the abnormal area in white condition.

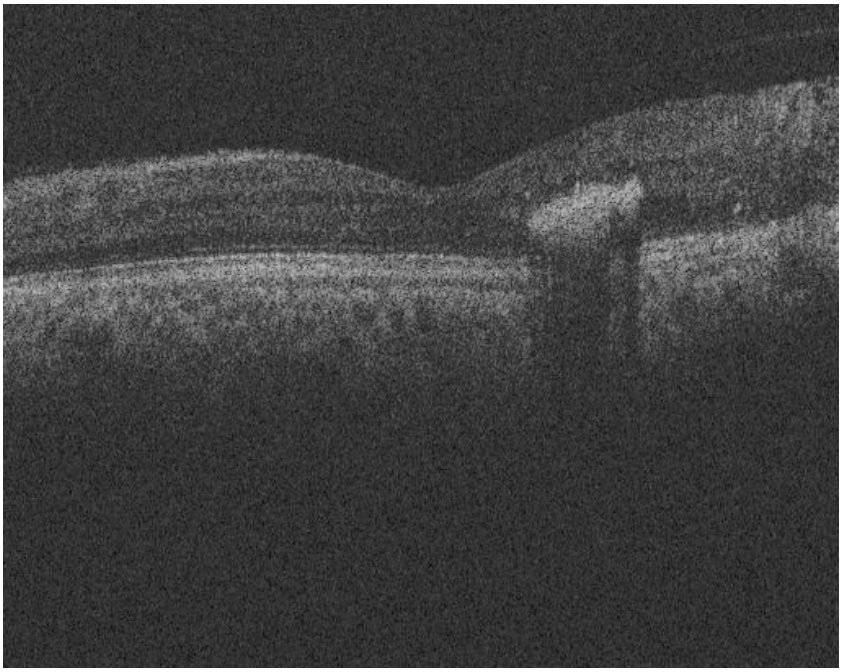

Figure 4.21 Original OCT retinal image – abnormal area in white condition

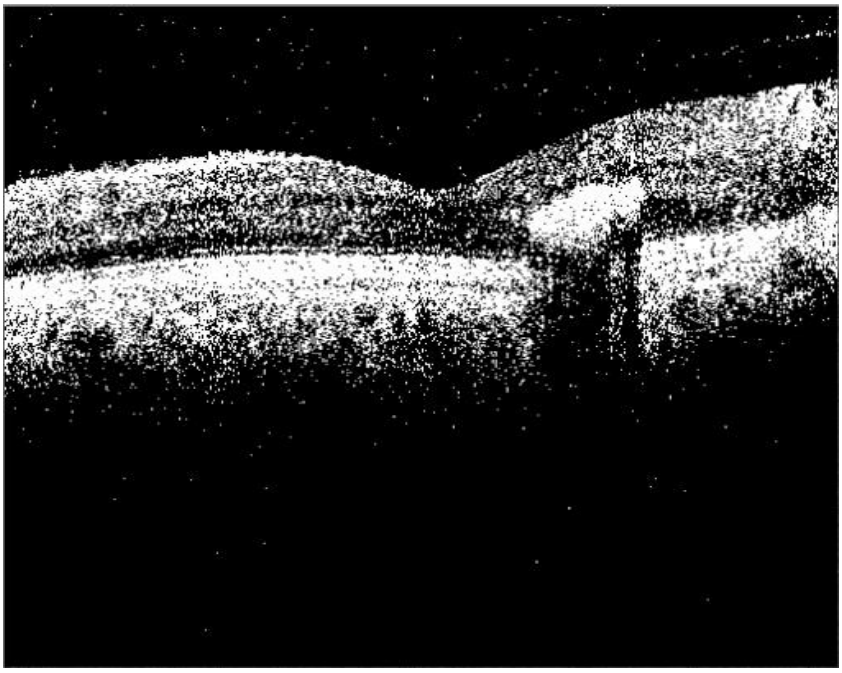

Figure 4.22 Binary image

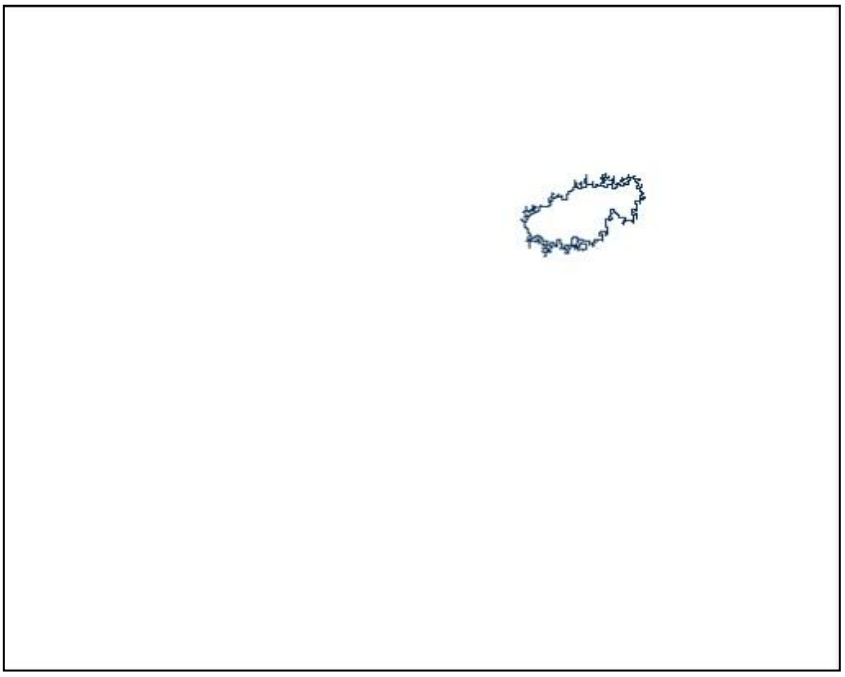

Figure 4.23 Border extraction image – using statistic border extraction method

Figure 4.22 shows the binary image. The original OCT image was changed to binary image directly without smoothing process. Even though Figure 4.23 shows the border extraction image extracted properly, there were some problems with this method. Firstly, this method was very sensitive. The changes value of standard deviation of gray value of ignition region, would changes the result. Figure 4.24 and Figure 4.25 show the different result compare to Figure 4.22 and Figure 4.23 even though used the same original image (Figure 4.21).

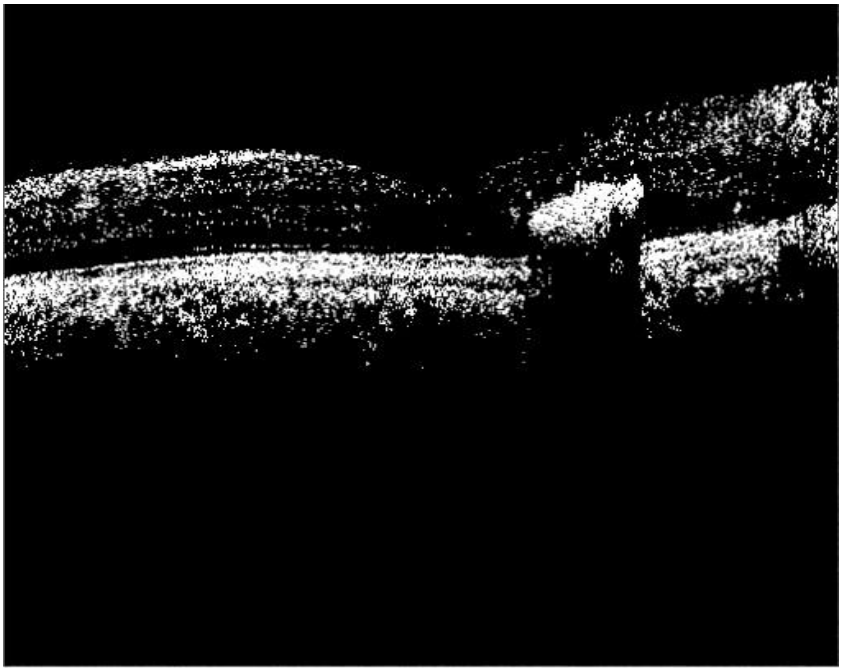

Figure 4.24 Binary image

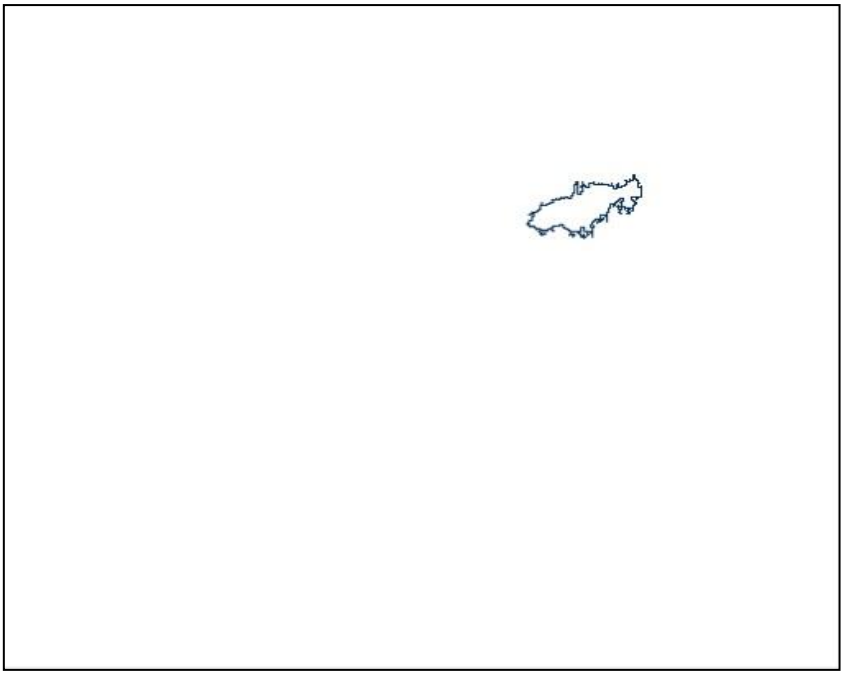

Figure 4.25 Border extraction image

There was a big different between Figure 4.23 and Figure 4.25 when the medical doctor selected the interested area at the different location in the abnormal

areal.

This method also cannot extract the abnormal area in OCT retinal image in black condition. Figure 4.26 shows the binary image result when this method was applied to OCT image contained the abnormal area in black condition.

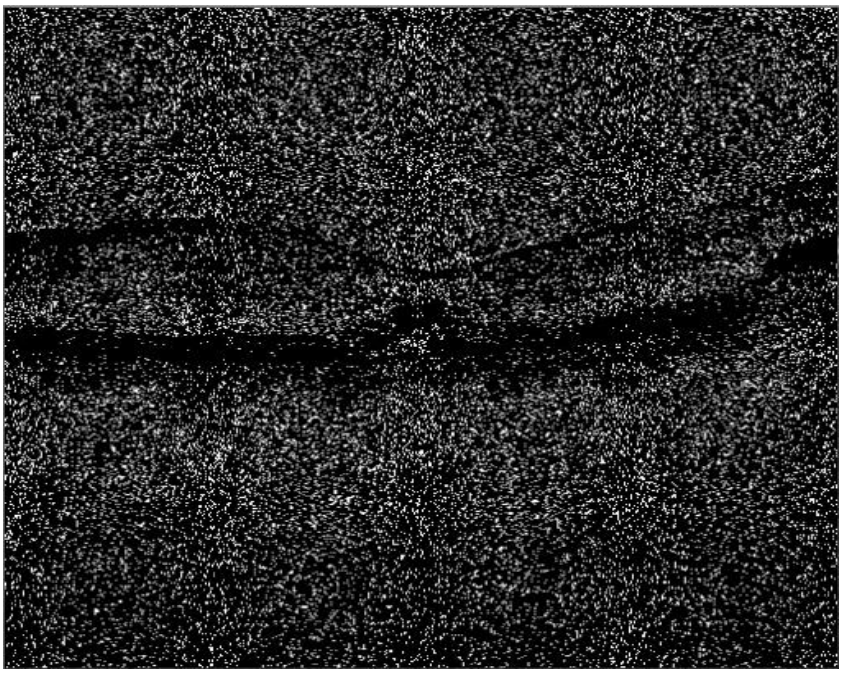

Figure 4.26 Binary image

From Figure 4.26, the method cannot extract any border of abnormal area.

4.4 REGIONAL STATISTICS AREA EXTRACTION METHOD

Regional statistic area extraction method (RSAEM) was proposed to extract the abnormal area in both black and white conditions. This method also could solve the problem of extracting the abnormal area in the damage condition of retinal layer. Equation (3.8) $(\sigma - a\sigma) < \sigma_x < (\sigma + a\sigma)$, the values of a was determined at 0.5, 1.0, 1.5,

and 2.0. Table 4.4 shows that the system has extracted the abnormal area from drusen OCT (abnormal area in black condition) image samples at the highest rate when *a* is set at 1.0. Table 4.5 shows that the system has extracted the abnormal area from DME OCT (abnormal area in white condition) image samples at the highest rate when *a* is set at 1.5.

Table 4.4 Extraction results from drusen OCT images using RSAEM

a (variable)	Extracted	Failed	Successful rate (%)
0.5	20	16	55.6
1.0	**26**	**10**	**72.2**
1.5	24	12	66.7
2.0	23	13	63.9

Table 4.5 Extraction results from DME OCT image using RSAEM

a (variable)	Extracted	Failed	Successful rate (%)
0.5	19	16	54.3
1.0	23	12	65.7
1.5	**26**	**9**	**74.3**
2.0	22	13	62.9

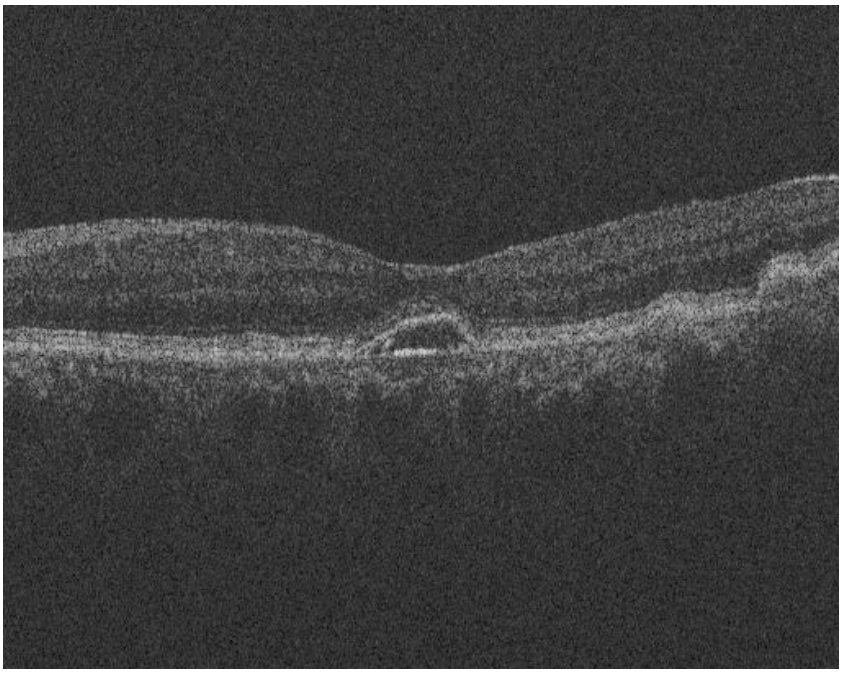

Figure 4.27 Original OCT image

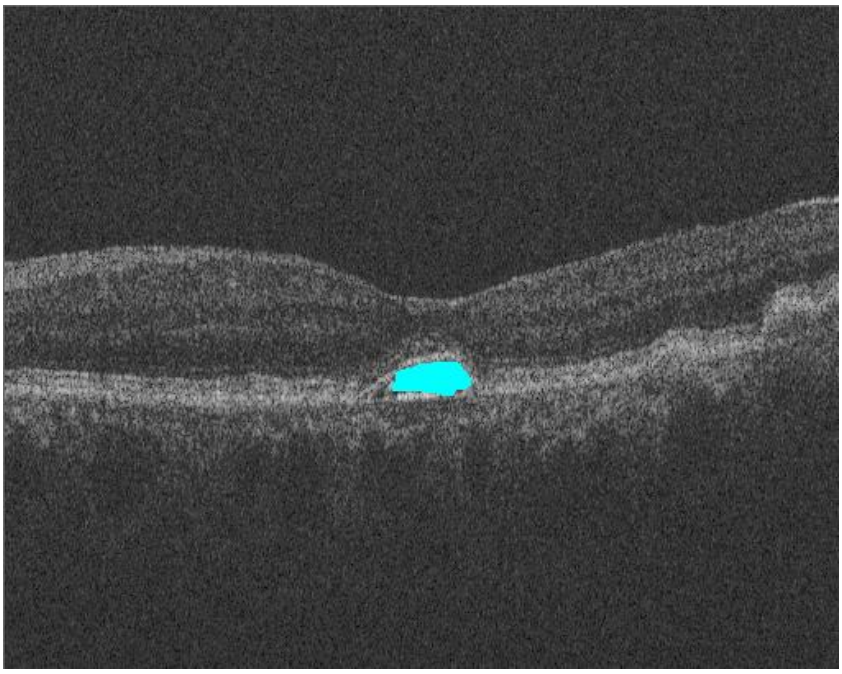

Figure 4.28 Extracted image using RSAEM

Figure 4.27 shows the abnormal area in original OCT image in black condition and Figure 4.28 shows the extracted image using RSAEM.

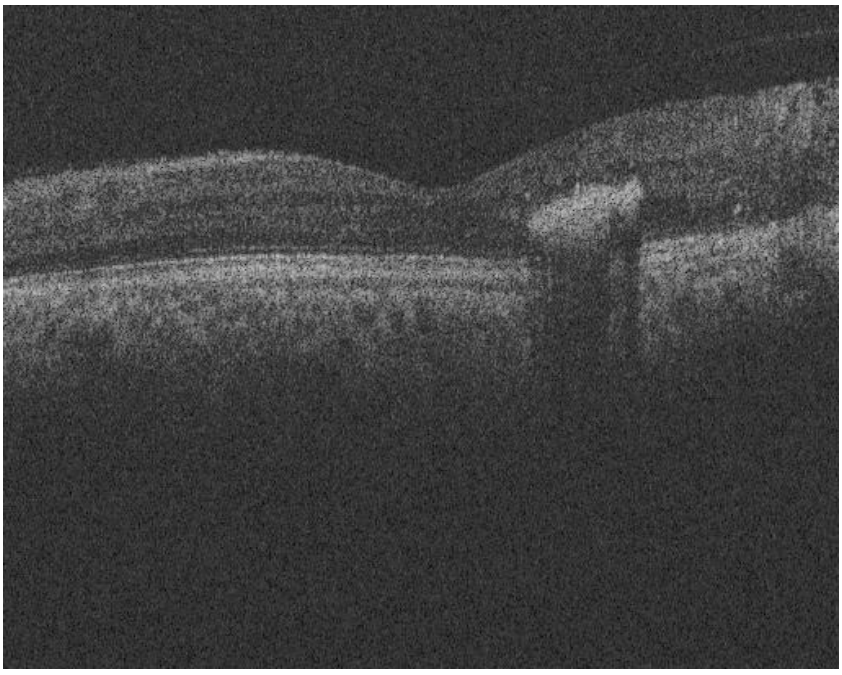

Figure 4.29 Original OCT image – abnormal area in white condition

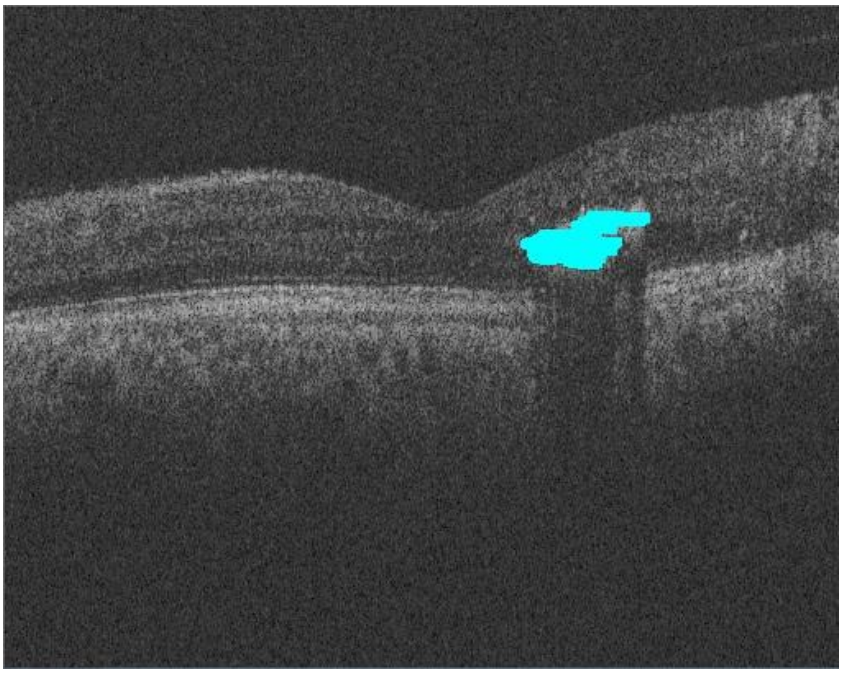

Figure 4.30 Extracted image using RSAEM

Figure 4.29 shows the abnormal area in original OCT image in white condition and Figure 4.30 shows the extracted image using RSAEM. Figure 4.31 shows that RSAEM has extracted the abnormal area from OCT image that contained damages at the retinal layer.

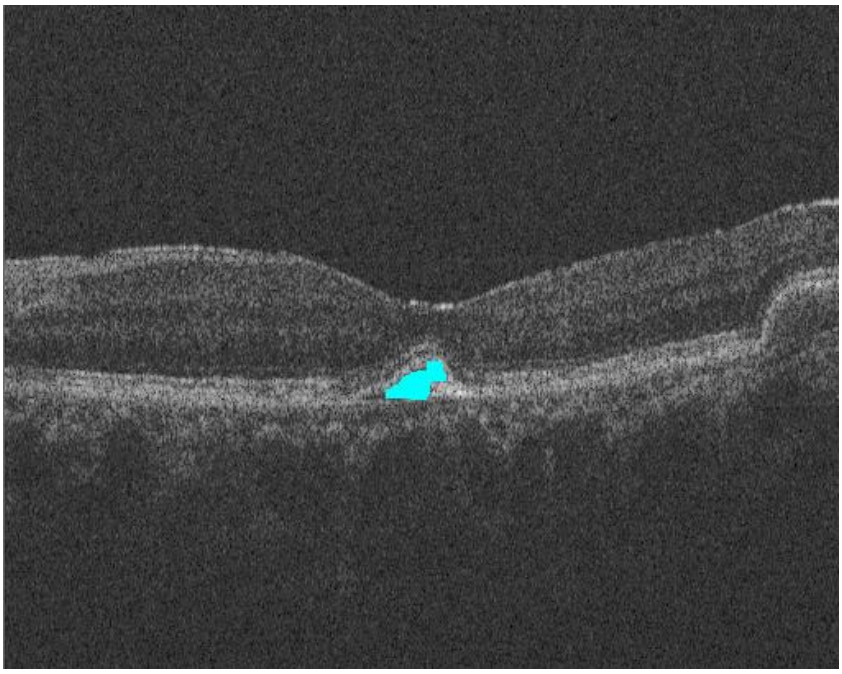

Figure 4.31 Extracted image using RSAEM

4.5 BORDER TRACKING PROCEDURE USING REGIONAL STATISTICS

Border tracking procedure using regional statistics (BTPRS) was proposed to improve RSAEM in extracting the abnormal area from OCT images. Using this method, original OCT image was changed to binary image before border tracking process started. From the Equation (3.9), the values of *a* was determined at 0.5, 1.0, 1.5, and 2.0. Table 4.6 shows that the system has extracted the abnormal area from drusen OCT image materials at the highest rate when *a* is set at 1.0. Table 4.7 shows that the system has

extracted the abnormal area from DME OCT image materials at the highest rate when *a* is set at 1.5.

Table 4.6 Extraction results from drusen OCT images using BTPRS

a (variable)	Extracted	Failed	Successful rate (%)
0.5	21	15	58.3
1.0	**28**	**8**	**77.8**
1.5	24	12	66.7
2.0	23	13	63.9

Table 4.7 Extraction results from DME OCT images using BTPRS

a (variable)	Extracted	Failed	Successful rate (%)
0.5	20	15	57.1
1.0	25	10	71.4
1.5	**28**	**7**	**80.0**
2.0	24	11	68.8

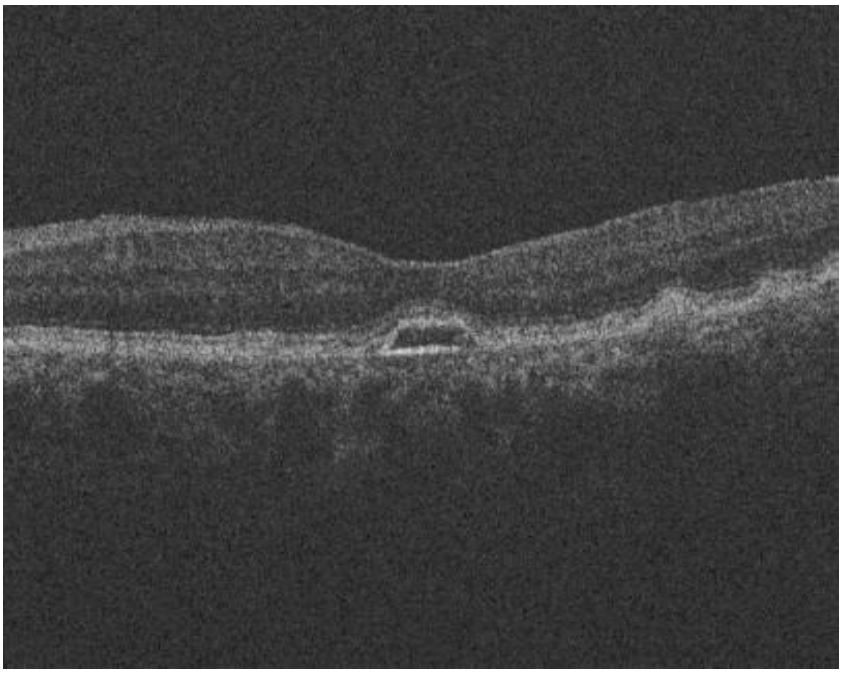

Figure 4.32 Original OCT image

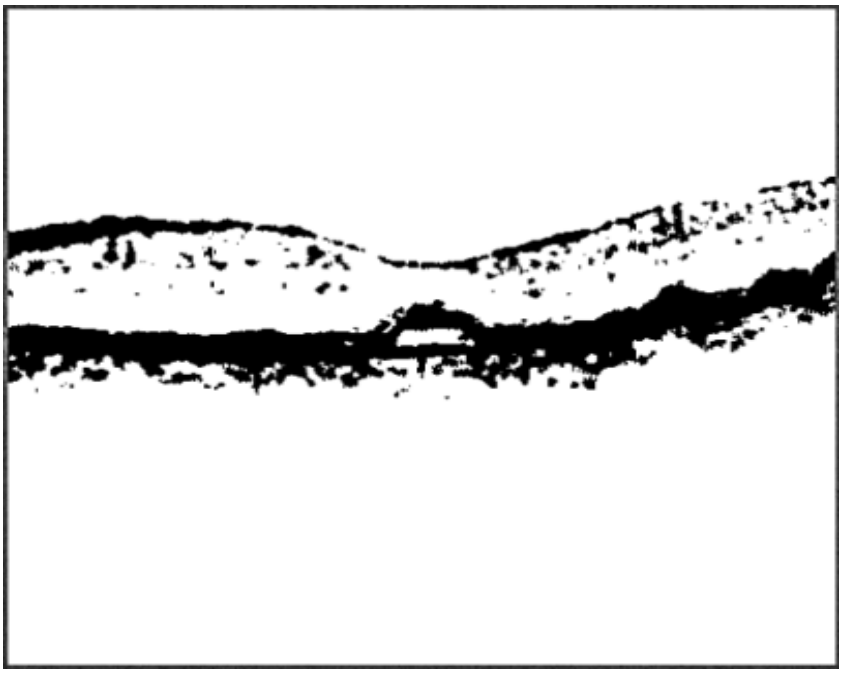

Figure 4.33 Binary image – extracted using BTPRS

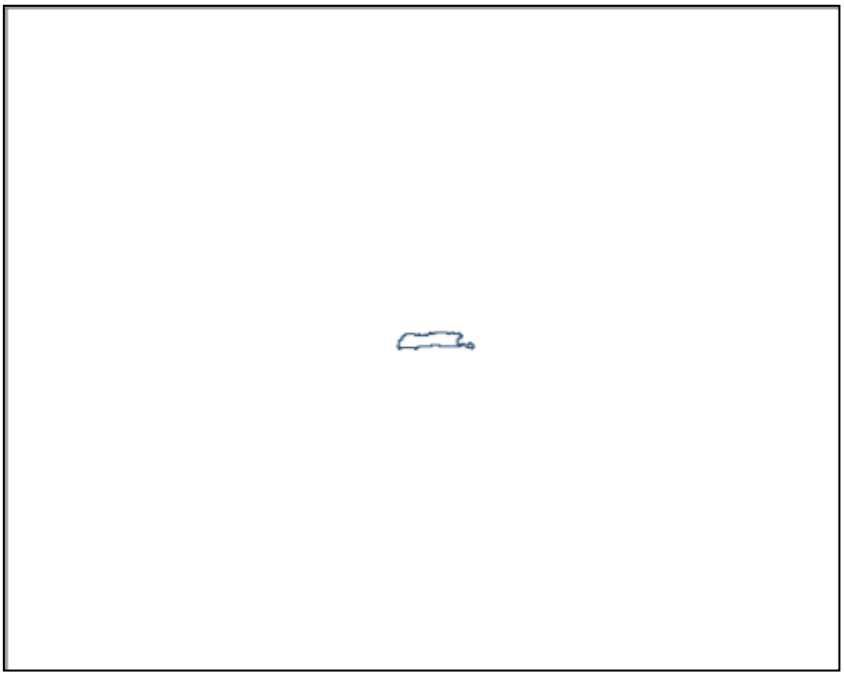

Figure 4.34 Border extraction image using BTPRS

Figure 4.32 shows the abnormal area in original OCT image in black condition and Figure 4.33 shows the binary image produced by using the BTPRS. Figure 4.34 shows the border extraction image, last output from BTPRS process.

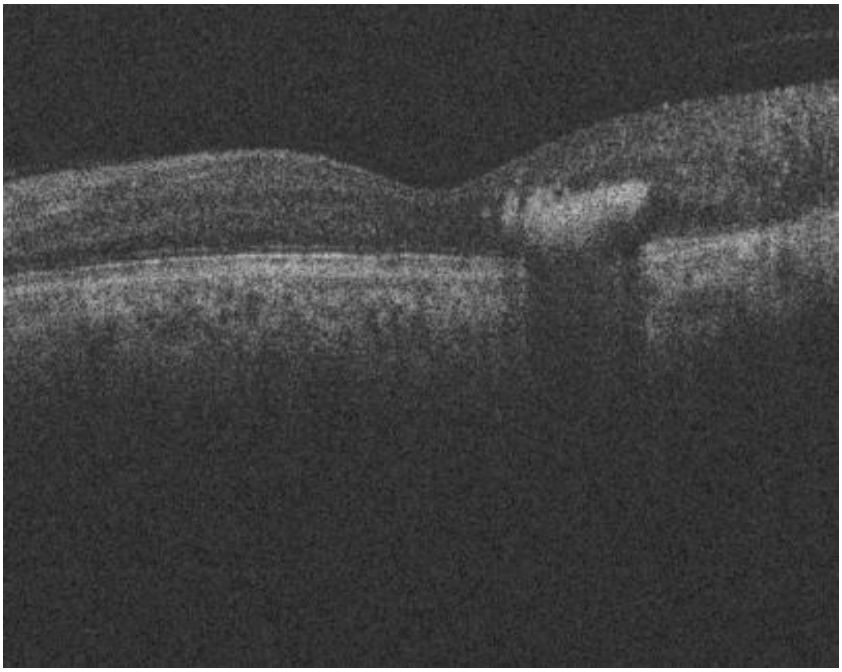

Figure 3.35 Original OCT image – abnormal area in white condition

Figure 3.36 Binary image – extracted using BTPRS

Figure 4.37 Border extraction image using BTPRS

Figure 4.35 shows the abnormal area in original OCT image in white condition and Figure 4.36 shows the binary image produced by using the BTPRS. Figure 4.37 shows the border extraction image, last output from BTPRS process.

4.6 COMPARISONS BETWEEN METHODS

Table 4.8 Comparisons the extraction rate between methods

Method	Image scanning	Border tracking	Statistics border tracking	RSAEM (highest)		BTPRS (highest)	
Percentage rate (%)	41.7	41.7	57.1	B	W	B	W
				72.2	74.3	77.8	80

From Table 4.8, the best method for this study is the border tracking procedure using regional statistics (BTPRS). Beside give the highest rate among the methods, BTPRS also can extract the abnormal area border in both conditions of OCT image. The extracted results more precise using BTPRS compare to RSAEM. Figure show the effectiveness the BTPRS compare to others methods. Original image number 74 from drusen material was tested in every method in this study. This image contained the damaged area at retinal layer. Image scanning method (see Figure 4.12) and border tracking method (see Figure 4.20) cannot extract the abnormal area properly. Even though the RSAEM can extract the abnormal area but the extracted result is not precise compare to the BTPRS method.

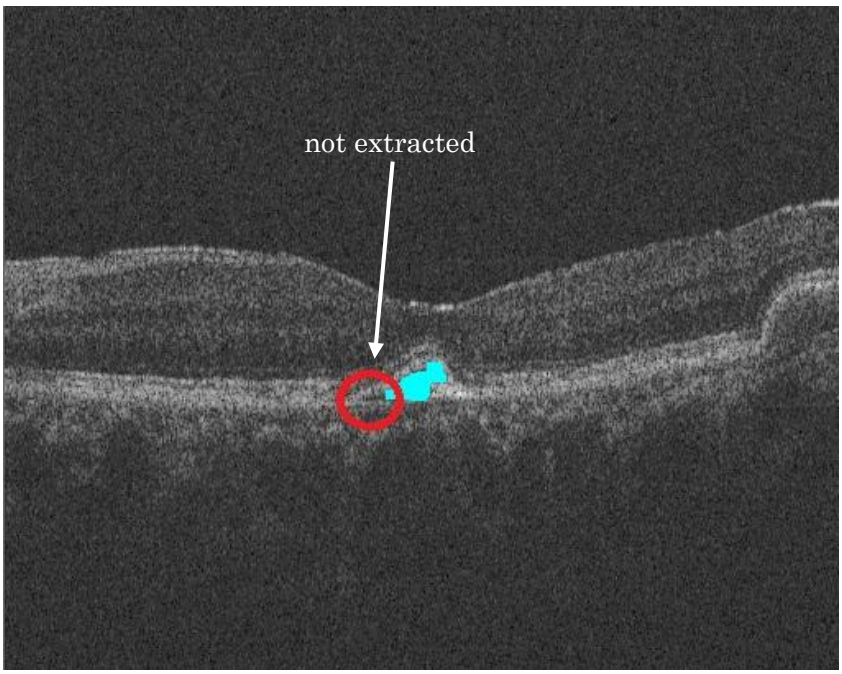

Figure 4.38 Extracted image using RSAEM

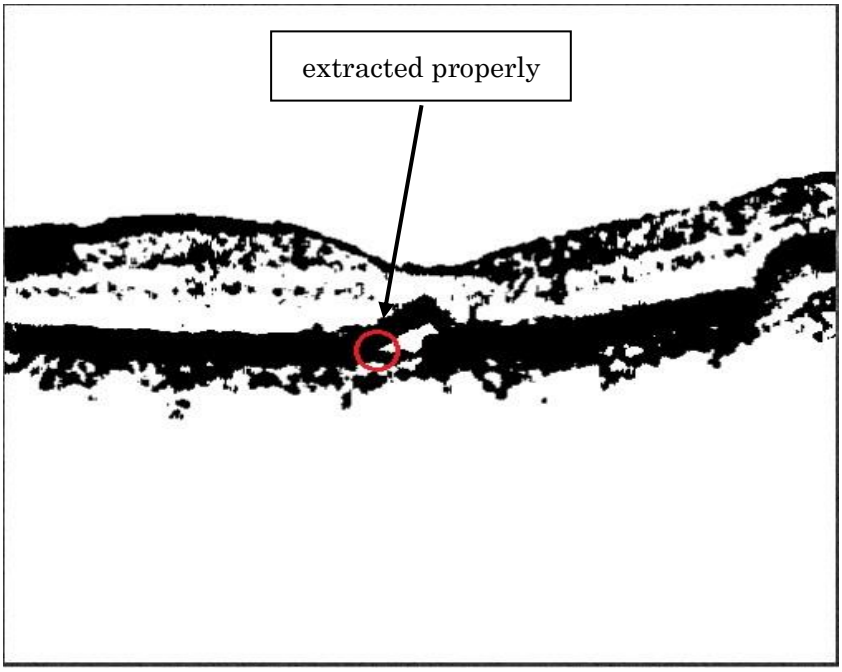

Figure 4.39 Smaller area extracted properly using BTPRS

Even though the BTPRS method can solve the problem in extracting abnormal area in the retinal layer structure, but in some cases it still need an improvement to get higher extraction rate. Figure 4.40 to 4.45 show the examples of extraction images from two different original OCT images. Figure 4.42 and Figure 4.45 show the final results from the BTPRS method. From Figure 4.40 to Figure 4.42, we can see the BTPRS method cannot extract half of the abnormal area when the area separated into two. The BTPRS method also cannot extract the abnormal area when the original image contained the bigger damage in the retinal layer (see Figure 4.43 to Figure 4.45)

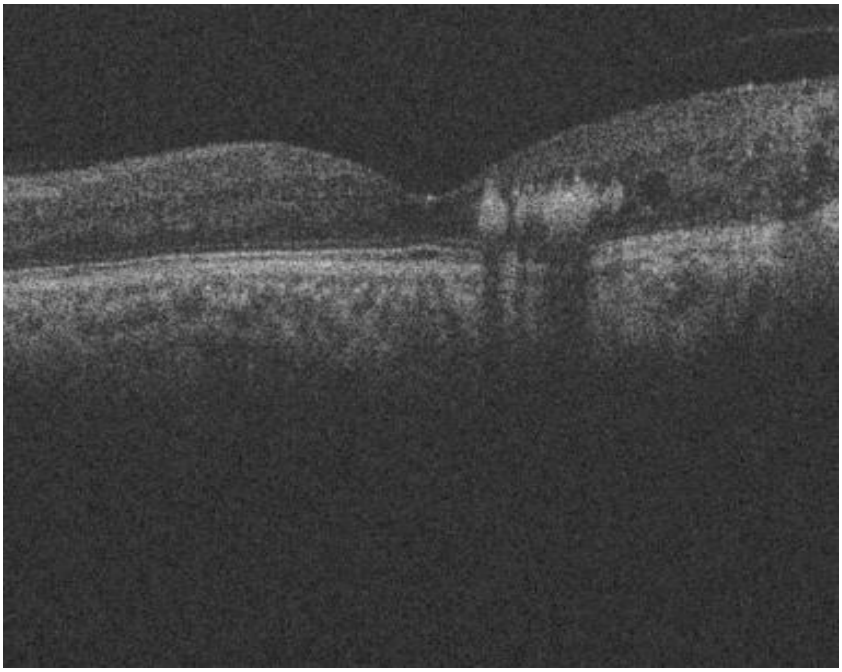

Figure 4.40 Original OCT image

Figure 4.41 Binary image

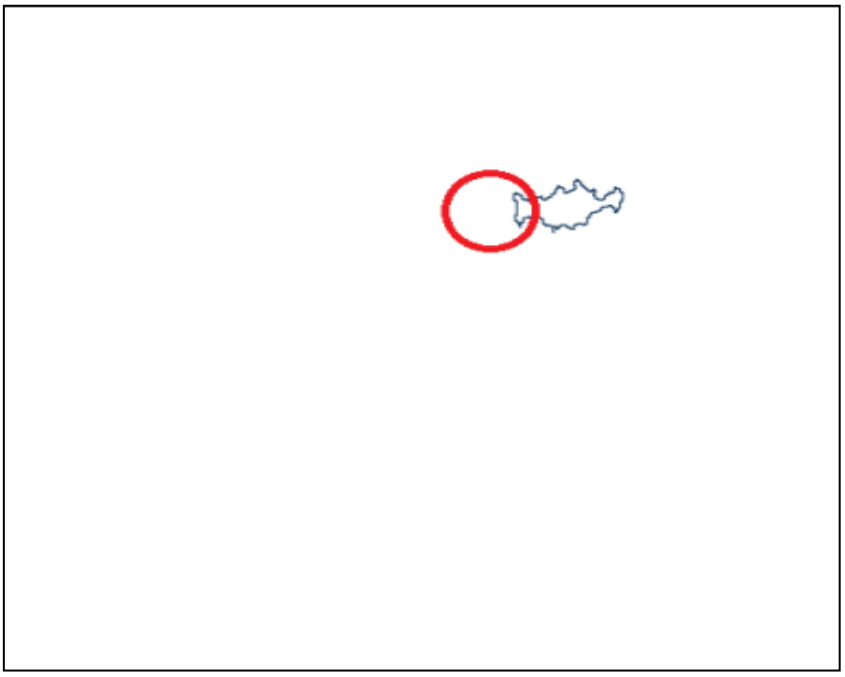

Figure 4.42 Border tracking image

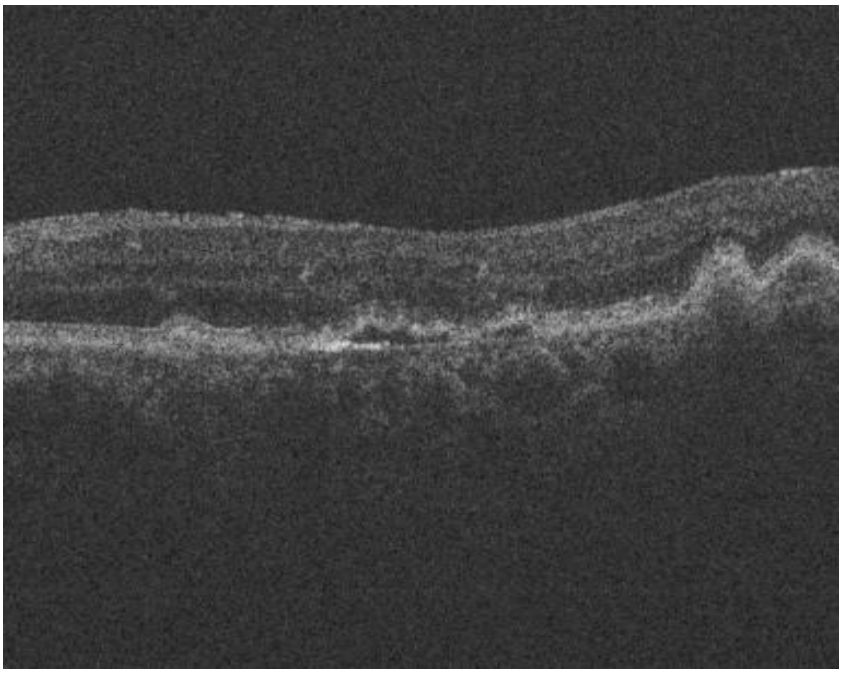

Figure 4.43 Original OCT image

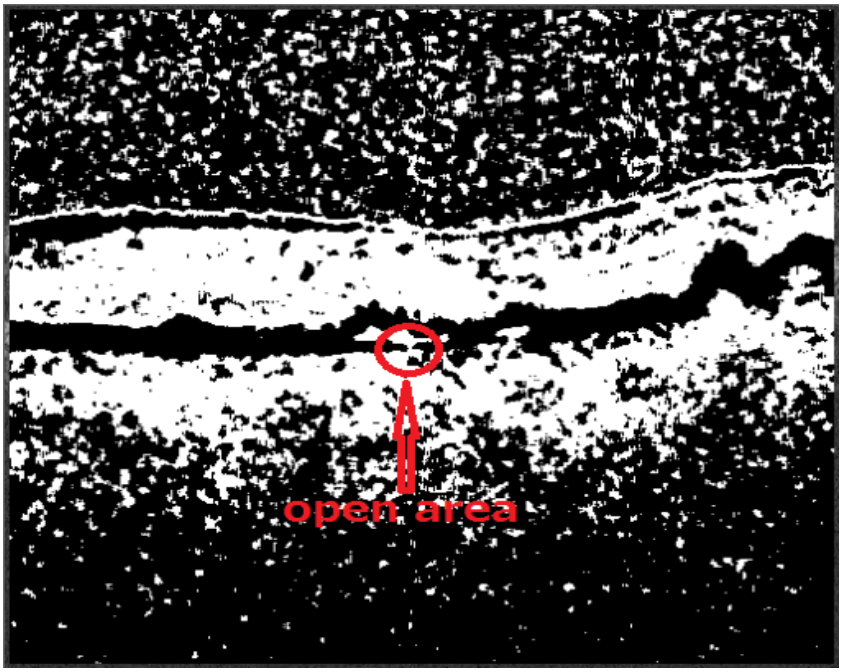

Figure 4.44 Binary image

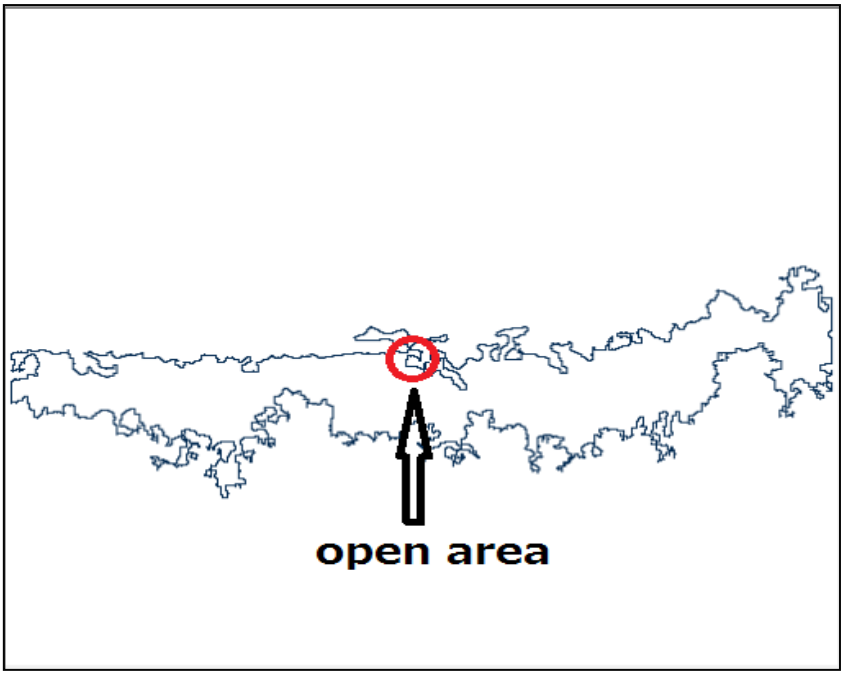

Figure 4.45 Border tracking image

CHAPTER V

CONCLUSION AND FUTURE WORKS

5.1 CONCLUSION

This research presented a new image processing algorithms for extraction of abnormal area from the human retina optical coherence tomography image. In this research, a comparison was made between different methods for extracting the abnormal area from selected images. The five methods used were

a. Image scanning method

b. Border tracking extraction method

c. Statistics border tracking method

d. Regional statistics area extraction method

e. Border tracking procedure using regional statistics method

The results from each method were compared and we found the border tracking procedure using regional statistics method provided the better extraction rate and more precise compare to other methods.

The first method used was image scanning method. The second method that we experimented with was the border tracking extraction method. Both of these methods posed similar problems that are

a. The methods cannot extract the abnormal area that contained the damage retinal layer in the OCT image.

b. The methods can extract the abnormal area in black condition only.

To overcome the problem and extract abnormal area in white condition from an OCT image, we proposed the third method, a new statistics border tracking method, which was used in the research. However, this method cannot extract the abnormal area existed in black condition.

In ensuring that we are able to extract the abnormal area from the retinal image, the research proposed and we used a new extraction method using regional statistics scanning image. This method can extract the abnormal area in both conditions white and black. To further improve the result of our research, we have proposed and used a new extraction method called border tracking procedure using regional statistics by combining both the regional statistics and border tracking methods.

It is then evident from all data and results gathered from the experiments, the border tracking procedure using regional statistic provides the best way to extract the abnormal area from human retinal optical coherence tomography images. This method is also able to extract the abnormal area from the OCT image existed both conditions, white or black. It also allows detection of any abnormal area specifically selected by a medical doctor.

5.2 SUGGESTIONS AND FUTURE WORKS

This research opens to further enhance the methods of obtaining sharper and more precise result for detecting abnormalities in OCT retinal images. In our opinion, another vanue worth experimenting to ensure more accurate result is by combining the mean and standard deviation values of every region and comparing them with the benchmark. It is our hope that this research will help the task of clinical doctors and the proposed computer aided diagnosis support system for OCT image at the present and future in detecting the degree of retina disease accurately.

REFERENCES

Bamber, J.C. & Tristam, M. 1988. Diagnostic Ultrasound. The Physics of Medical Imaging (ed. Webb, S.). 319 – 388. Adam Hilger, Bristol and Philadelphia.

Bille, J.F., Drehe, A.W. & Zinser, G. 1990. Scanning Laser Tomography of the Living Human eye. in Noninvasive Diagnostic Techniques in Ophthalmology. (ed. Master, B.R.). 528–547. Springer Verlag, New York.

Bowd, C., Weinreb, R.N., Williams, J.M. & Zangwill, L.M. 2000. The Retinal Nerve Fiber Layer Thickness in Ocular Hypertensive, Normal and Glaucomatous Eyes with Optical Coherence Tomography. Arch. Ophthalmol. 118:22–26.

Drexler, W., Morgner. U., Ghanta, R.K., Kartner, F.X., Schuman, J.S., Fujimoto, J.G., 2001. Ultrahigh-resolution Ophthalmic Optical Coherence Tomography. Nature Medicine. Vol. 7. No 4:502-7.

Fercher, A. F., 1996. Optical Coherence Tomography. Journal of Biomedical Optics 1(2):157 –173.

Fercher, A. F., Hitzenberger, C. K., Drexler, W., Kamp, G., Sattmann, H. 1993 Ophthalmol. 116:113.

Fujimoto, J. G., Pitris, C., Boppart, S.A., Brezinski, M.E., 2000. Optical Coherence Tomography: An Emerging Technology for Biomedical Imaging and Optical Biopsy. Neoplasia, Vol. 2, Nos 1-2:.9-25.

Gass, J. D. M. 1997. Macular. In Stereoscopic Atlas of Macular Disease: Diagnosis and Treatment. 1:1-49. (Mosby, St. Louis, Missouri).

Gonzalez, R. C. & Woods, R. E., 2001. Digital Image Processing. 2nd ed. Prentice Hall. New Jersey.

H. K. Tony, J. G. Fujimoto, J. S. Schuman, L. A. Paunescu, A. M. Kowalevicz, I. Hartl, W. Drexler, G. Wallstein, H. Ishikawa, J. S. Duker. 2005. Comparision of Ultrahigh and Standard Resolution Optical Coherence Tomography for Imaging Macular Pathology. Ophthalmology, Vol 112.11:1922-35.

Huang, D. et al. 1991. Optical Coherence Tomography. Science 254:1178–1181.

Kodama, D., Yamakawa, A., Tsuruoka, S., Kawanaka, H., Takase, H., Kadir, M. F. A., Matsubara, H., Okuyama, F. 2010. A Retinal Layer Structure Analysis to Measure The Size of Disease Using Layer Boundaries Detection for Optical Coherence Tomography Images. World Congress Biomechanics, International Federation for Medical and Biological Engineering. 1554-7.

Kouichi, S. 2007. Digital Image Processing: Basic and Applied. (in Japanese). CQ Publisher. Japan

Krebs, W. & Krebs, I. 1991. Primate Retina and Choroid – Atlas of Fine Structure in Man and Monkey. 4–8. (Springer, New York).

Master, B.R. & Thaer, A.A. 1994. Real-time Scanning Slit Confocal Microscopy of the In Vivo Human Cornea. Appl. Opt. 33:695–701.

ORBIS. 2003. Interpretation of Stereo Ocular Angiography: Retinal and Choroidal Anatomy.
http://telemedicine.orbis.org/bins/content_page.asp?cid=1-8989-8993-9001
[28 June 2012].

Pascolini D., Marioti S. P., Dec 2011. Global estimates of Visual Impairment 2010. *British Journal Ophthalmology Online*. 10.1136/bjophthalmol-20110300539.

Pavlin, C.J., McWhae, J.A., McGowan, H.D. & Foster, F.S. 1992. Ultrasound Biomicroscopy of Anterior Segment Tumors. Ophthalmology. 99:1220–1228.

Puliafito, C.A., Hee, M.R., Schuman, J.S. & Fujimoto, J.G. 1995. in Optical Coherence Tomography of Ocular Disease. Slack, Thorofare, New Jersey.

Rao, S. R., Mohabi, H., Yang, A. Y., Sastry, S. S. & Ma, Y. 2009. Natural Image Segmentation with Adaptive Texture and Boundary Encoding. Visual Computing Group Microsoft Research Asia.

Sakaue, K., Yamamoto, K. 1991. Active Net Model and Its Application to Region Extraction. The Journal of the Institute Television Engineers of Japan. Vol 44. 10:1155–1163.

Schuman, J. S., Puliafito, C. A., Fujimoto, J. G. 2004. Optical Coherence Tomography of Ocular Disease. 2nd Ed. (Slack Inc., Thorofare, NJ).

Swanson, E. 2009. Ophthalmic Optical Coherence Tomography Market: Past, Present, & Future Optical Coherence Tomography News. http://www.octnews.org/articles/1027616/ophthalmic-optical-coherence-tomography-market-pas [20 June 2012].

VisionRx. 2005. Encyclopedia – Macula. Eye Care Library. http://www.visionrx.com/library/enc/enc_macula.asp [27 July 2012].

WHO. 2012. Visual Impairment And Blindness. World Health Organization. http://www.who.int/mediacentre/factsheets/fs282/en/index.html [29 June 2012].

Webb, R.H., Hughes, G.W. & Pomerantzeff, O. 1980. Flying Spot TV Ophthalmoscope. Appl. Opt. 19:2991-2997.

Yagi, T., Okuyama, F., Kawanaka, H., Tsuruoka, S. 2008. A Study on Extraction Method of Internal Limitting Membrane and Retina Pigment Epithelium from OCT Images. SCIS & ISIS. 2008-13.

Yamakawa, A., Kodama, D., Tsuruoka, S., Kawanaka, H., Takase, H., Kadir, M. F. A., Matsubara, H., Okuyama, F. 2010. Extraction Method of Retinal Border Lines in Optical Coherence Tomography Image By Using Dynamic Contour Model. World Congress Biomechanics, International Federation for Medical and Biological Engineering. 1558-61.

Zaimer, R., Asrani, S., Zou, S., Quigley, H. & Jampel, H. 1998. Quantitative Detection of Glaucomatous Damage at the Posterior Pole by Retinal Thickness Mapping. 1Ophthalmology. 105:224–231.